

A TRANSISTORIZED SPHERICAL POLARCARDIOGRAPH

by

PATRICK JOHN RONALD HARDING

B.A.Sc., The University of British Columbia, 1959

A THESIS SUBMITTED IN PARTIAL FULFILMENT OF
THE REQUIREMENTS FOR THE DEGREE OF
MASTER OF APPLIED SCIENCE

in the Department of
Electrical Engineering

We accept this thesis as conforming to the
required standard

THE UNIVERSITY OF BRITISH COLUMBIA

May, 1963

In presenting this thesis in partial fulfilment of the requirements for an advanced degree at the University of British Columbia, I agree that the Library shall make it freely available for reference and study. I further agree that permission for extensive copying of this thesis for scholarly purposes may be granted by the Head of my Department or by his representatives. It is understood that copying or publication of this thesis for financial gain shall not be allowed without my written permission.

Department of

Electrical Engineering

The University of British Columbia,
Vancouver 8, Canada.

Date

May 7 1963

ABSTRACT

The design of a two-dimensional polarcardiograph and the use of two such two-dimensional devices to calculate the third polar coordinate together with the circuitry necessary to derive and amplify a set of voltages proportional to the Cartesian coordinates x , y , and z is described.

Although the technique used for obtaining the polar coordinates is similar to that used in other instruments, the circuitry is somewhat different. This is dictated in part by the fact that this device is completely transistorized.

Both the Frank and ~~RAFE~~ networks are available for the transformation from patient signals to a set of signals proportional to the Cartesian coordinates x , y , and z .

Restoration of the base-line at the optimum time during the cardiac cycle is achieved through a system of gated feedback which is activated by a predictor circuit. The predictor is triggered by an automatic trigger selector.

A threshold circuit is associated with each angle output in order to set the output to some predetermined value when the input signal level is so small as to make the angle output indeterminate.

ACKNOWLEDGEMENT

The author would like to thank Dr. A.D. Moore, the supervising professor, for his help and guidance throughout this research project and Dr. G.E. Dower whose research has demonstrated that a transistorized polarcardiograph would be useful in electrocardiography. The author is also indebted to the technicians in the Electrical Engineering shop for their assistance on this project.

The principal part of this research was carried out under the National Research Council Block Term Grant BT-68. Additional assistance was given under a grant from the British Columbia Heart Foundation.

TABLE OF CONTENTS

	Page
LIST OF ILLUSTRATIONS	iv
ACKNOWLEDGEMENT	vi
1. Introduction	1
2. Principle of the Computer	6
3. Amplifiers and Lead-system Networks	12
4. Base-line Clamping	16
4.1 General Description	16
4.2 The Automatic Trigger Selector	20
4.3 The Clamp Advance Circuit	22
5. The Two-dimensional Computer	26
5.1 General Description	26
5.2 The Multipliers	26
5.3 The Carrier Generator	28
5.4 The Low-pass Filter	31
5.5 Magnitude Detection	33
5.6 Angle Detection (phase comparison)	35
5.7 The Clipper	36
5.8 The Threshold Circuit	37
6. The Three-dimensional Computer	40
7. Test Results	42
8. Conclusions	49
Appendix	50
References	63

LIST OF ILLUSTRATIONS

Figure		Page
1.1	Coordinate systems in electrocardiography .	2
1.2	Types of electrocardiograms	3
2.1	Two-dimensional trigonometric computer	7
2.2	Three-dimensional trigonometric computer ..	9
3.1	Amplifying and clamping circuit	14
4.1	Typical electrocardiographic waveform	17
4.2	Clamp system used in the previous polar- cardiograph	18
4.3	Clamp system used in this polarcardiograph	19
4.4	Automatic trigger selector	21
4.5	Clamp advance circuit	23
4.6	Waveforms generated in the clamp advance circuit	24
5.1	Block diagram of the two-dimensional trigonometric computer as constructed	27
5.2	Circuit diagram of a multiplier	28
5.3	Carrier generator output waveforms	29
5.4	4-Kc carrier generator	30
5.5	Waveforms used to ensure correct phasing of carrier generator outputs	32
5.6	Low-pass filter	33
5.7	Low-pass filter response curves	34
5.8	Waveforms of the phase comparator	35
5.9	Waveforms of the threshold circuit	37
5.10	Block diagram showing the threshold control circuit	39
6.1	Block diagram of the three-dimensional polarcardiograph	41

	Page
7.1	Plot of detected output as a function of input for the two-dimensional computer . 44
7.2	Plot of detected output as a function of input for the three-dimensional computer .. 45
7.3	Recording of angle outputs of the two-dimensional computer for three different peak-to-peak input-signal levels, (a) 15 volts, (b) 4 volts, (c) 0.8 volts 46
7.4	Recording of polar angle output of the three-dimensional computer for three different peak-to-peak input-signal levels, (a) 15 volts, (b) 4 volts, (c) 0.8 volts .. 47
7.5	Recording of angle output of the two-dimensional computer showing threshold circuit in operation for four different threshold levels, (a) 10%, (b) 3%, (c) 1.5% 48
A.1	Circuit diagram for preamplifiers 53
A.2	Circuit diagram for second and third stage amplifiers 54
A.3	Circuit diagram for Frank and RAFE lead systems 55
A.4	Circuit diagram of coupling network and relays 56
A.5	Circuit diagram for automatic trigger selector 57
A.6	Circuit diagram for clamp advance circuit . 58
A.7	Circuit diagram for two-dimensional computer 59
A.8	Circuit diagram for 4-Kc carrier generator 60
A.9	Circuit diagram for threshold control 61
A.10	Circuit diagram for frontal magnitude detector and polar-axis delay 62

1. INTRODUCTION

The instrument to be described here is an analogue computer which converts electrical signals proportional to the Cartesian coordinates x , y , and z into electrical signals proportional to the plane and spherical polar coordinates r , R , ϕ , and θ . The relationship between these coordinates is shown in Figure 1.1. Such a computer finds an application in electrocardiography since voltages proportional to the Cartesian coordinates x , y , and z of a "heart vector" can be obtained by the proper arrangement of electrodes on a patient's body.

The heart produces an electric field within the body varying in direction and magnitude throughout the cardiac cycle. This field gives rise to potential differences between points on the surface of the body. Continuous recordings of such voltages on a time scale are called electrocardiograms (Figure 1.2). In present-day electrocardiography, a dozen electrocardiographic recordings are usually taken, one after another, from a number of electrode positions. As a first approximation, the heart's electric field may be considered to arise predominantly from a single current dipole.¹⁻³ The dipole moment is known as the heart vector. The simplification which the heart-vector concept allows cannot ordinarily be utilized in clinical electrocardiography because it is impossible to reconstruct the vector accurately from the usual electrocardiograms even though they may be considered to arise from it.

A much more accurate picture of the heart vector is

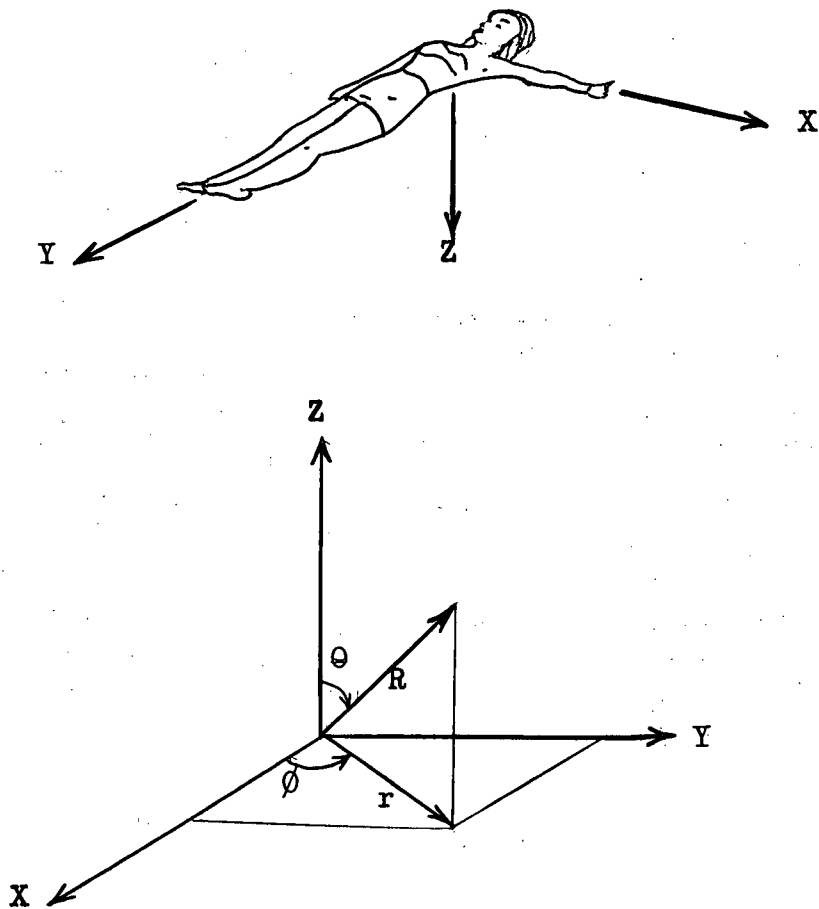


Figure 1.1 Coordinate system in electrocardiography

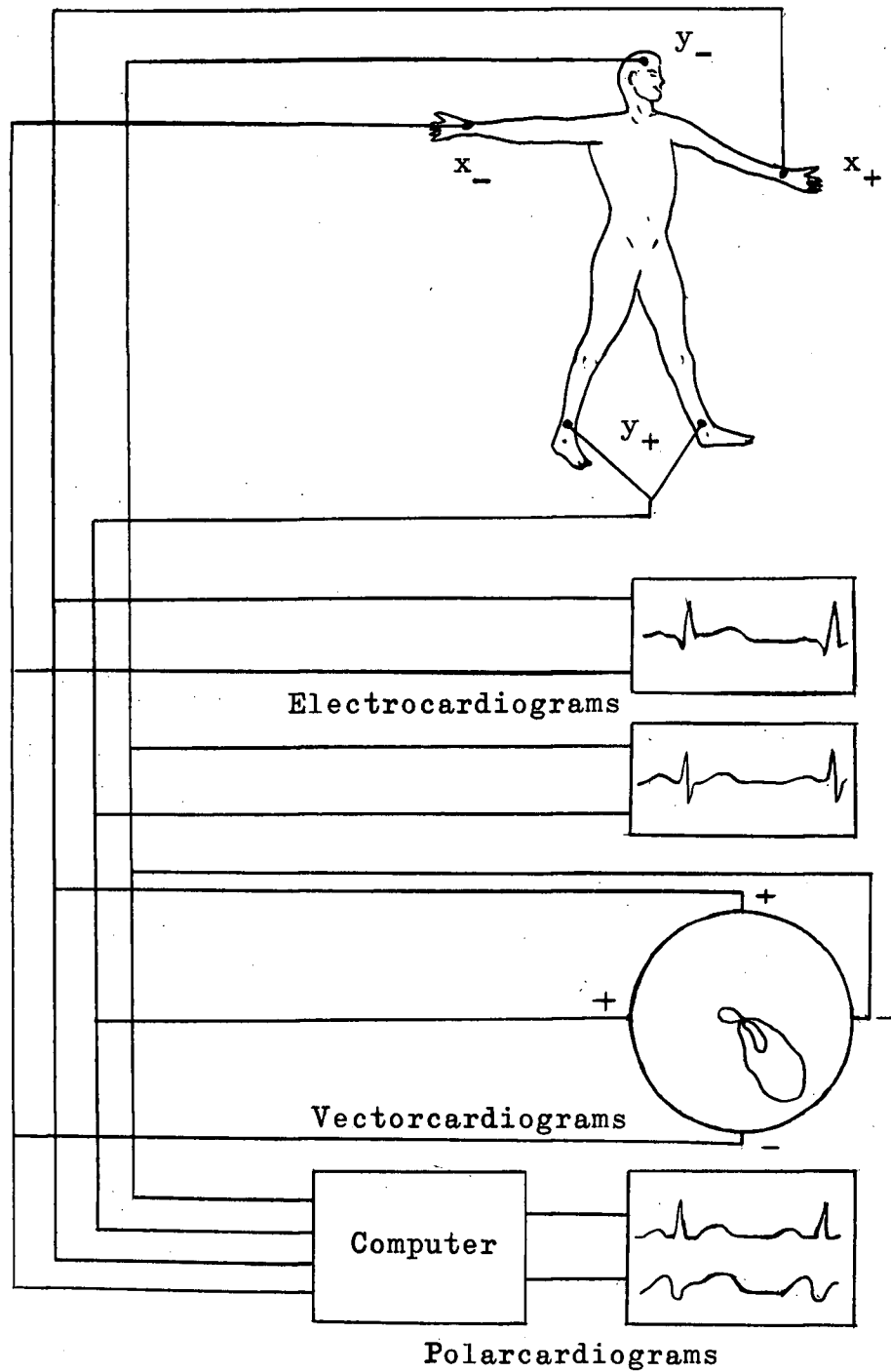


Figure 1.2 Types of electrocardiograms

obtained by applying orthogonal lead signals to the horizontal and vertical plates of a cathode-ray tube and photographing the locus of the spot during one heart cycle. This two-dimensional projection of the heart vector is called a vectorcardiogram (Figure 1.2).³ The same technique can be used in three dimensions by stereoscopic presentation.⁴

Vectorcardiograms suffer from the disadvantage that the electrical phenomena they record are not displayed on a time scale. This leads to loss of detail around the origin and vagueness concerning the temporal relationship between parts of the vectorcardiogram and certain elements in the electrocardiogram which are clinically important.

Another way to display electrocardiographic data is to record the polar coordinates of the heart vector on a time scale. Such recordings are known as polarcardiograms (Figure 1.2).⁵

Despite a continued interest in trigonometric computers for this use,⁶⁻⁸ the only polarcardiograph that has performed successfully under clinical conditions has been the one developed in this laboratory. However, the development and clinical trial of this device have suggested several possibilities for improvement. These are as follows:

- (1) Increase in input resistance to reduce the effects of skin resistance and thus simplify the technique of electrode application.

- (2) Improvement in base-line clamping to compensate automatically for variations in heart rate, and automatic selection of clamp triggering signal.

(3) Simultaneous recording of spherical polarcardiograms using three different choices of polar axis.

(4) Removal of indeterminate angle outputs associated with small magnitudes by a threshold control circuit.

(5) Obtaining magnitude and direction outputs when the heart vector is parallel to the polar axis.

This thesis describes the design and construction of an improved polarcardiograph embodying the above features. The use of transistors and printed circuits together with improvements in design makes possible a considerable reduction in physical size as well as an improvement in reliability and ease of servicing.

2. PRINCIPLE OF THE COMPUTER

The basic operating principle of this polarcardiographic computer is similar to that used in other versions of the instrument.^{5,9,10} Two voltages proportional to the orthogonal components of a vector in two dimensions are multiplied by corresponding quadrature sinusoids of unit amplitude and the outputs are summed. The angle of the vector can be found by comparing the phase of the waveform vector with that of one of the quadrature carrier signals, while the envelope of the waveform is proportional to the magnitude of the vector. Two such trigonometric computers can be combined to give the angle and magnitude of a vector in three dimensions.

A simple version of a two-dimensional trigonometric computer is shown in Figure 2.1. The orthogonal set of voltages proportional to the Cartesian coordinates x and y are related to the polar coordinates r and ϕ as follows:

$$x = r \cdot \cos \phi \quad (2.1)$$

$$y = r \cdot \sin \phi \quad (2.2)$$

$$r = \sqrt{x^2 + y^2} \quad (2.3)$$

$$\phi = \tan^{-1} y/x \quad (2.4)$$

The plane polar coordinates r and ϕ can be obtained in the following manner. The input signals x and y are multiplied by quadrature sinusoids v_1 and v_2 , giving

$$v_1 x = r \cdot \cos \phi \cdot \sin \omega t \quad (2.5)$$

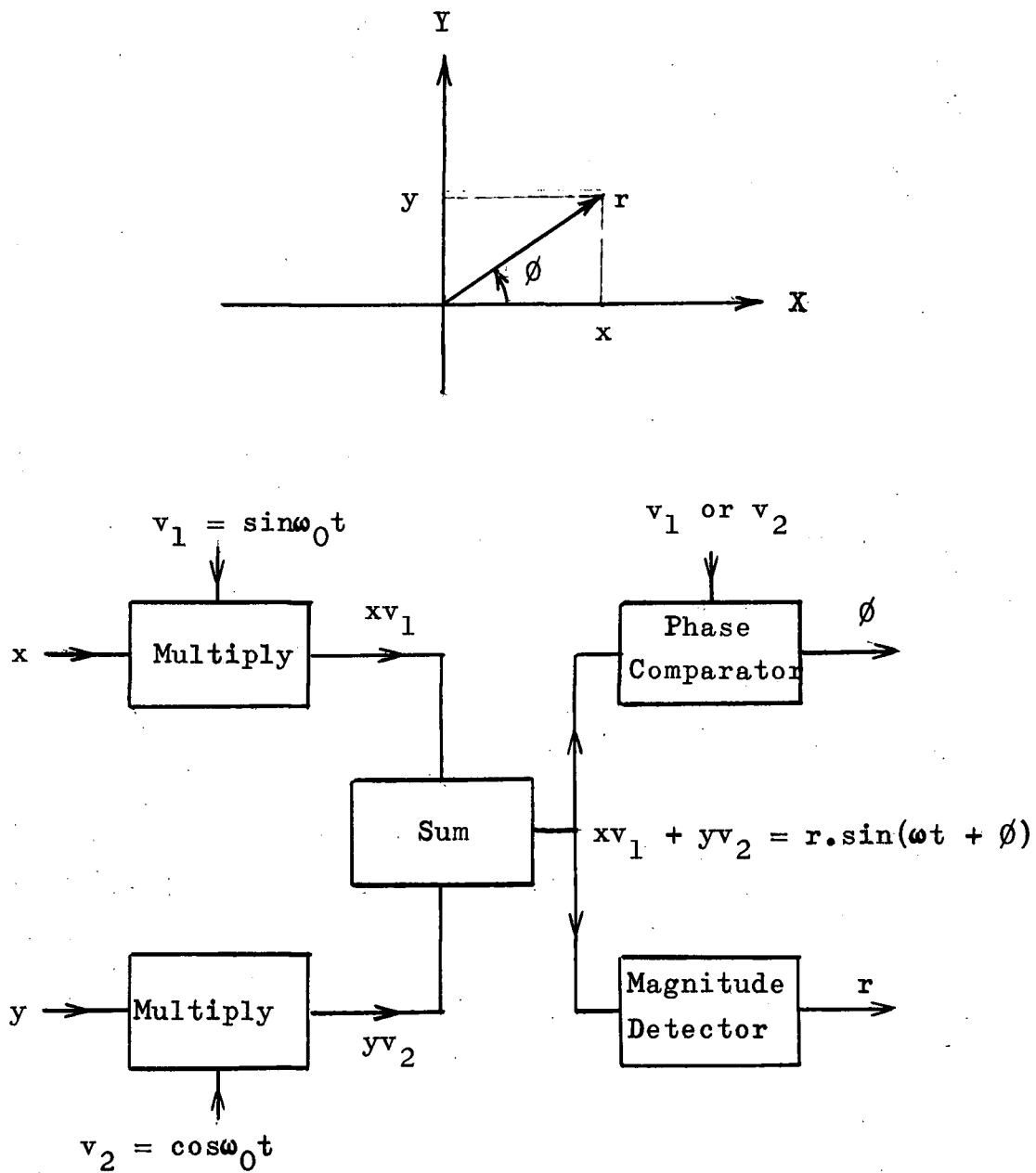


Figure 2.1 Two-dimensional trigonometric computer

$$v_2y = r \cdot \sin\phi \cdot \cos\omega t \quad (2.6)$$

Adding Equations 2.5 and 2.6 yields

$$\begin{aligned} v_1x + v_2y &= r \cdot (\cos\phi \cdot \sin\omega t + \sin\phi \cdot \cos\omega t) \\ &= r \cdot \sin(\omega t + \phi) \end{aligned} \quad (2.7)$$

A voltage proportional to the angle ϕ is obtained by comparing the phase of the waveform $r \cdot \sin(\omega t + \phi)$ with that of v_1 or v_2 . A voltage proportional to r , the magnitude of the vector, is extracted from this waveform by envelope detection.

The polar coordinates of a vector in three dimensions can be computed by combining two two-dimensional trigonometric computers as shown in Figure 2.2. The magnitude output, r , of the first computer is used as one of the orthogonal inputs to the second computer. A voltage proportional to the third Cartesian coordinate, z , is the other input. The inputs to the second computer are related to the polar coordinates as follows:

$$r = R \cdot \sin\theta \quad (2.8)$$

$$z = R \cdot \cos\theta \quad (2.9)$$

Solving for R and θ yields

$$\begin{aligned} R &= \sqrt{r^2 + z^2} \\ &= \sqrt{x^2 + y^2 + z^2} \end{aligned} \quad (2.10)$$

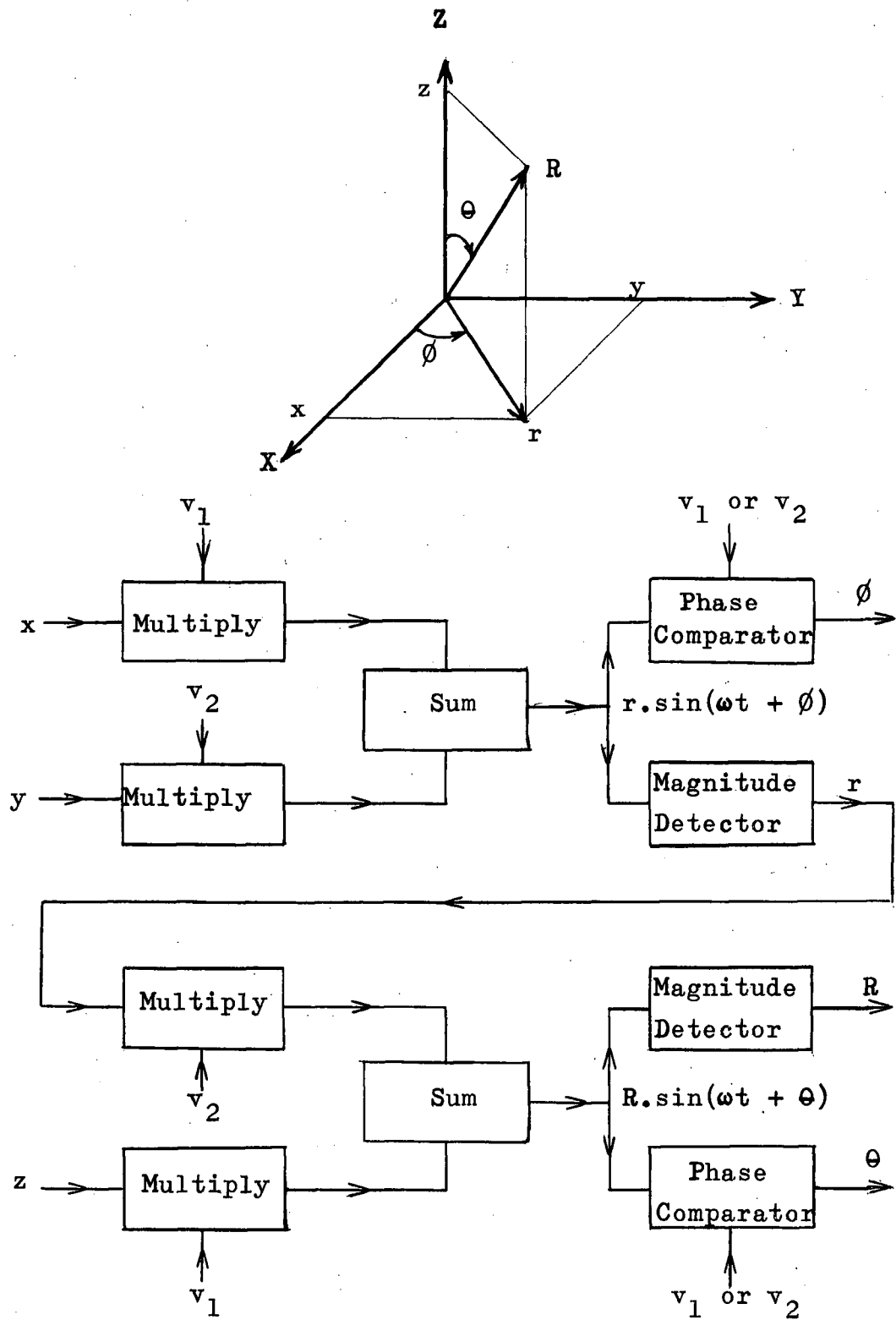


Figure 2.2 Three-dimensional trigonometric computer

and $\theta = \cot^{-1} z/R$ (2.11)

The two spherical polar coordinates, R and θ , are found by first multiplying r and z by the quadrature sinusoids v_1 and v_2

$$v_1 z = R \cdot \cos \theta \cdot \sin \omega t \quad (2.12)$$

$$v_2 r = R \cdot \sin \theta \cdot \cos \omega t \quad (2.13)$$

Adding Equations 2.12 and 2.13 gives

$$\begin{aligned} v_1 z + v_2 r &= R \cdot (\sin \theta \cdot \cos \omega t + \cos \theta \cdot \sin \omega t) \\ &= R \cdot \sin(\omega t + \theta) \end{aligned} \quad (2.14)$$

Voltages proportional to the spherical polar coordinates R and θ are obtained from the summed multiplier outputs as before.

The instrument to be described here is made up of two two-dimensional trigonometric computers of the type above, except that square waves are substituted for the sinusoids (see Chapter 5). The coordinates (r, ϕ) of the projection of the heart vector in the x - y plane are given by the frontal computer. The remaining two polar coordinates (R, θ) are provided by the polar computer.

Standard electrocardiographic lead systems do not ordinarily give x, y, and z directly. However, linear combinations of the voltages obtainable from the patient can be used to derive x, y, and z by means of resistive summing networks. Because the fluctuations in the potential differences being observed are of the order of one millivolt, and because there may in addition be a large dc bias due to electrode polarization, it will be necessary to amplify the signals and to eliminate the dc component before analogue computation is done. The following chapter will describe the amplifiers and resistive networks used.

3. AMPLIFIER AND LEAD-SYSTEM NETWORKS

A circuit which will derive and amplify analogue voltages proportional to the Cartesian coordinates x , y , and z to the level of ten volts needed by the multipliers must meet the following nine requirements:

(1) The circuit should contain a resistive network which will transform voltages available at the patient into a set of voltages proportional to the Cartesian coordinates x , y , and z .^{11,12} Although it is possible to use a set of patient leads to derive these voltages directly, this raises difficulties because it requires electrode positions which are not easy to locate or are inconvenient. It is more satisfactory to place electrodes at easily located positions on the body (e.g. left leg, right arm, centre of chest, etc.) and to derive the analogue signals x , y , and z by linear combination of the electrode voltages. The function of the lead-system networks is to carry out this transformation.

(2) The circuit must have high input resistance in order that the effect of patient skin resistance be small. Because the patient skin resistance is sometimes as high as 50 kilohms, the input resistance should be several megohms.

(3) Because transistors are to be used, it is necessary that the first stage of amplification in this circuit be fed from a low-resistance source so that the noise level will be low.

(4) The average input signal is of the order of one millivolt, thus requiring an overall voltage amplification of ten thousand.

(5) The inputs to all amplifier stages should be differential to give high in-phase rejection in order that the circuit be relatively insensitive to 60-cycle pick-up and to power-supply variations.

(6) The circuit should remove the large dc bias normally present in the low-level signals so that this bias will not tend to block the amplifiers.

(7) The output terminals of the circuit should have an average dc level close to zero volts to suit the requirements of the multipliers to be used.

(8) The multipliers also require that the output circuit have a low internal resistance.

(9) The circuit should be capable of re-establishing the zero level or base-line of the analogue output signals once during each heart cycle.

The circuit shown in Figure 3.1 was designed to meet the above specifications when using as many as eight patient electrodes, including a ground electrode. It can be seen from this diagram that by inserting the resistive networks before the preamplifiers, four amplifiers could have been eliminated, but this was not feasible because of the conflicting conditions imposed by requirements (2) and (3). That is, if the resistive networks had been designed to give a high input resistance, then the source resistance as seen by the first stage of

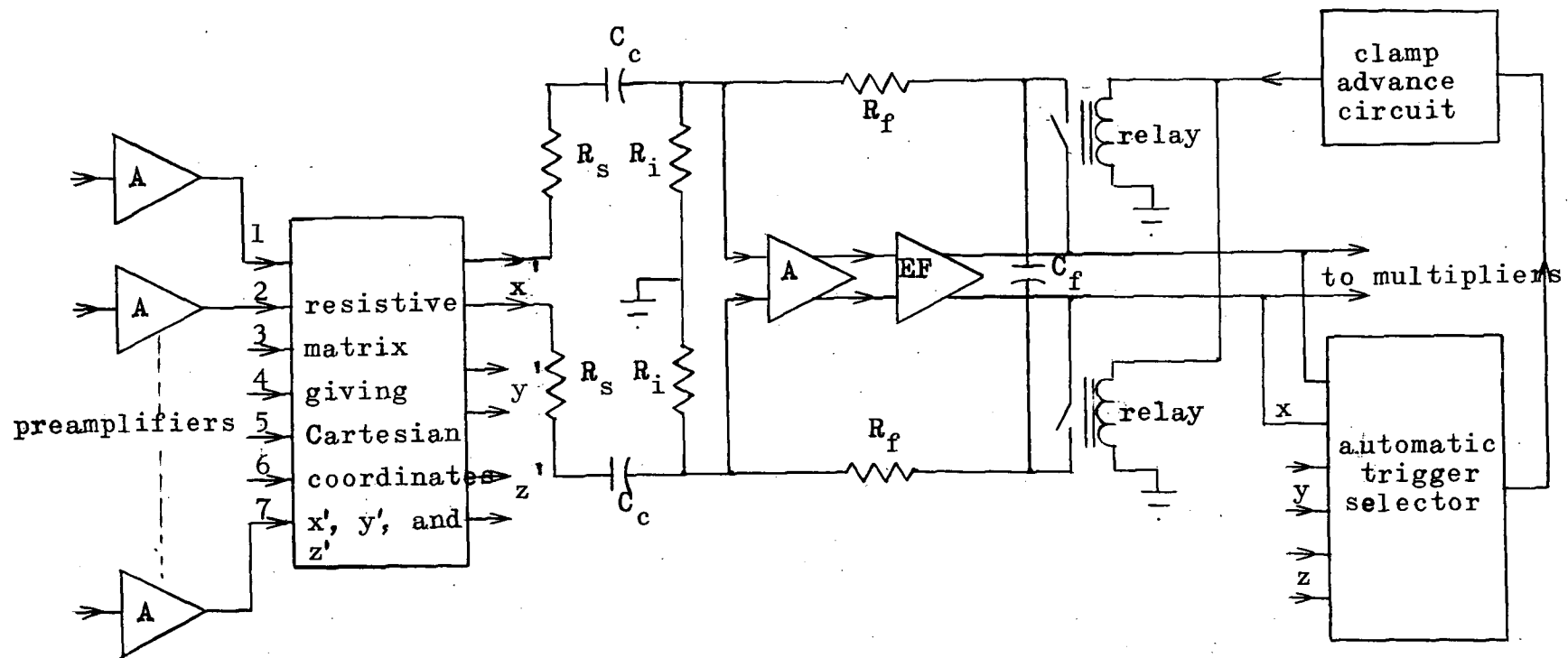


Figure 3.1 Amplifying and clamping circuit

amplification would have been very high and would have given rise to a high noise level.

The seven input amplifiers, as well as the three second-stage amplifiers shown, are of the differential configuration described by Hilbiber¹³ (Figures A.1 and A.2). The input resistance of an amplifier is of the order of two megohms and the voltage amplification is equal to 100.

Two alternative resistive networks are used here (Figure A.3), one for the Frank lead system,¹¹ requiring seven patient electrodes, and the other for the RAFE system,¹² requiring only four. These networks are designed in such a way that the internal resistance seen at any output terminal is 100 kilohms (the original Frank Network has been modified to achieve this). The input resistance of these networks is approximately two to three times this value.

The dc bias is removed from the low-level signals by RC coupling between the first two stages of amplification, giving a lower half power-frequency of approximately 0.08 cycles per second.

Compound emitter followers in conjunction with zener diodes (Figure A.2) are used to give the required low-resistance output and zero average dc potential at the output terminals.

The requirement that the circuit re-establish the base-line of the analogue output signals once during each heart cycle is fulfilled by using relays to give gated feedback once during each cycle. This feedback arrangement is described in detail in the following chapter.

4. BASE-LINE CLAMPING

4.1 General Description

In the transformation from Cartesian to polar coordinates shown in Figure 1.1, it is important to define the origin of the system. Although the waveforms in Cartesian coordinates are only affected in average value by the position of the origin, it is apparent that the equivalent polar coordinates are much more dependent upon the position of the origin.

The most natural choice for the origin is that which lets $x = y = z = 0$ during the resting interval of the heart cycle (Figure 4.1), when the electrical activity of the heart is assumed to be zero. Because of the use of RC-coupled amplifiers, the average value of x , y , and z at the output of the amplifiers is not zero relative to the resting level. Hence, it is necessary to restore the base-line regularly by base-line clamping during each heart beat.

In the original polarcardiograph, the base-line was re-established by connecting together the input grids of an RC-coupled amplifier during the resting interval of each cycle, (Figure 4.2).⁵ The time constant of the coupling circuit, $(R_s + R_i)C_c$, was made large in order to hold the bias established.

In the clamp system used in this instrument, the base-line is maintained by using gated feedback to reset the output to zero during the clamp interval and to establish a bias voltage on C_f which tends to be maintained until the next clamp

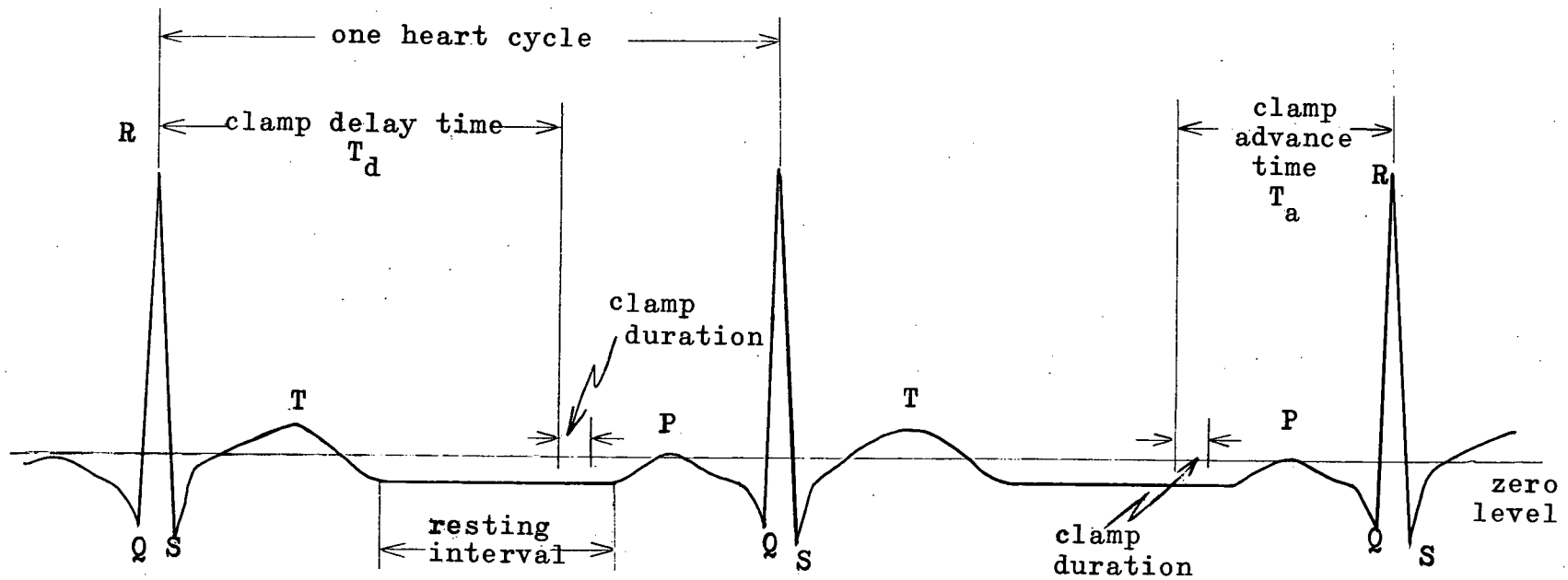


Figure 4.1 Typical electrocardiographic waveform

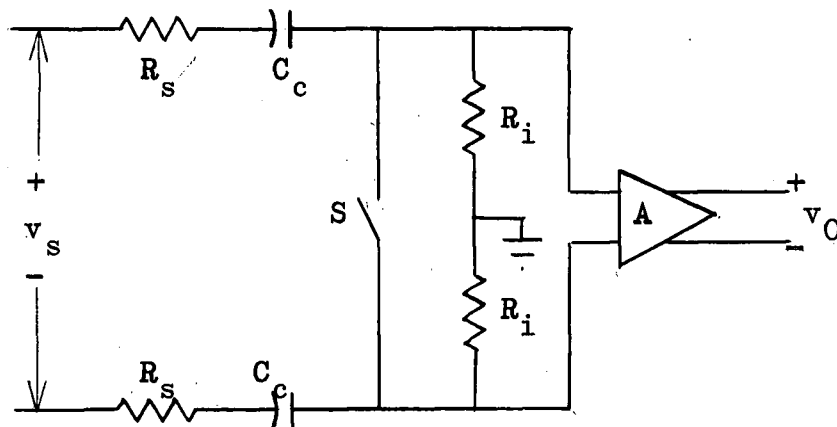


Figure 4.2 Clamp system used in the previous polar-cardiograph

interval (Figure 4.3). The elements R_i , R_s , R_f , C_c , and C_f in this circuit are so proportioned that the transient voltage on the amplifier input terminals due to the bias established on C_f decays with a long time constant and with zero initial slope when the relays open.

In the previous instrument, the relays were triggered in the following manner. The QRS portion of one of the six waveforms x , $-x$, y , $-y$, z , and $-z$, was selected by the operator and used to trigger a delay circuit which in turn actuated the relays after an adjustable interval, the clamp delay time T_d in Figure 4.1. This system did not prove entirely satisfactory because of the frequency with which the operator

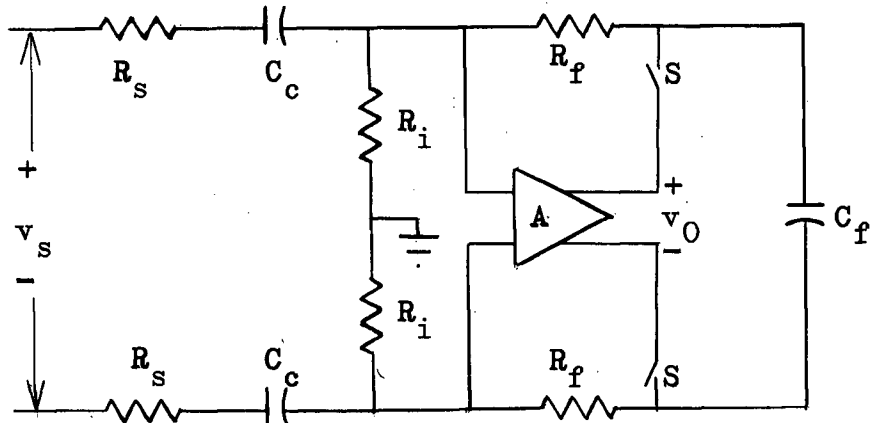


Figure 4.3. Glamp system used in this polarcardiograph

had to readjust the controls. The period of the heart cycle can change over a relatively short interval of time, and the operator had to readjust the clamp delay, not only from patient to patient, but during the course of a recording. The clamp trigger system to be described here is designed to lessen, and in most cases to eliminate, the adjustments required because of these variations.

The principal effect on heart waveforms due to a change in heart rate is in the duration of the resting interval (Figure 4.1).¹⁴ This fact has been used in the design of the present system, so that clamping tends to occur at a preset time, T_a , in advance of the instant when the QRS complex

has its greatest rate of change, rather than at a preset time after this instant as in the previous instrument. This is done by anticipating the occurrence of the next trigger pulse, on the basis of the known value of the preceding period, and clamping at the preset time before that pulse.

Although it is expected that this new system of clamp triggering will be a considerable convenience in the majority of cases, unforeseen difficulties may arise in occasional cases with complicated cardiac rhythms. For this reason, the original system of clamp triggering is available to the operator as an alternative.

4.2 The Automatic Trigger Selector

The circuit shown in Figure 4.4 is used to identify the occurrence of the greatest slope of the three component waveforms. This is done on the basis of the greatest positive slope of the six waveforms; x , $-x$, y , $-y$, z , and $-z$. These signals are differentiated and fed into amplifiers biased beyond cutoff. The six output pulses consisting of negative-going spikes relative to the collector supply voltage (12 volts), drive an OR-gate through emitter followers. The output of the OR-gate is shunted with a large capacitor (2 microfarads), and the maximum voltage appearing across the capacitor will be equal to that of the largest spike, which coincides with the greatest slope of the QRS complex. The capacitor will discharge through the shunt resistor, R_1 , between QRS complexes. If the minimum difference between the maximum spike and the next largest is greater than the decay in capacitor voltage during one cycle, then the charging current for each cycle will be only

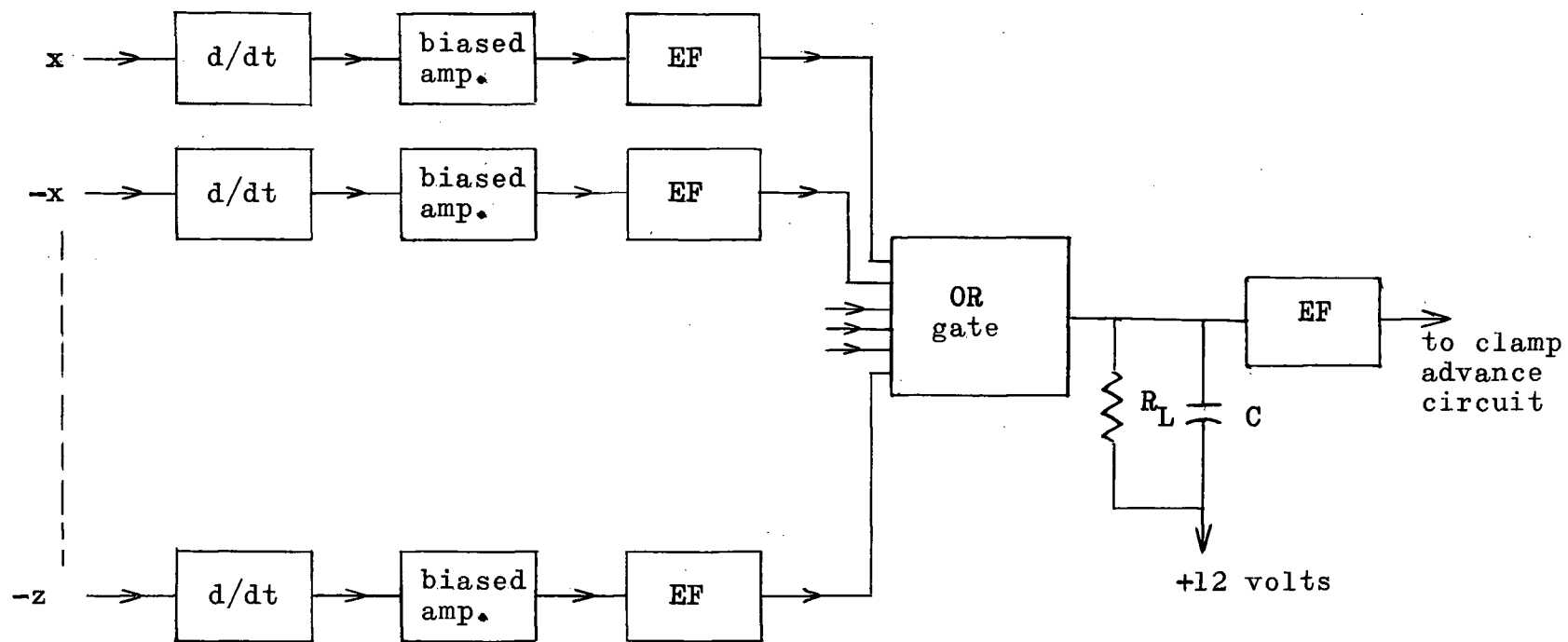


Figure 4.4 Automatic trigger selector

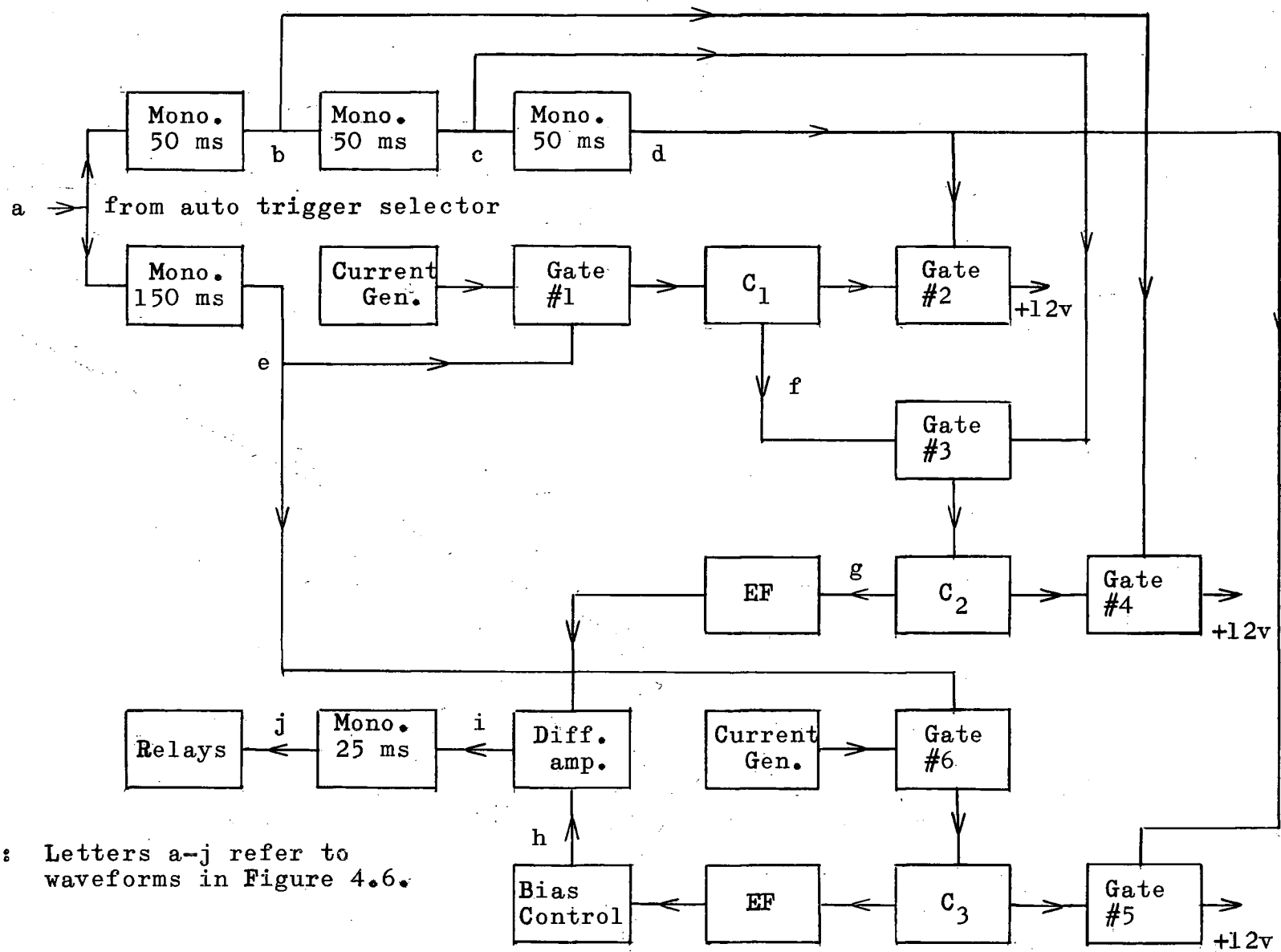
that produced by the largest spike. The capacitor voltage is applied to an emitter follower and the "discontinuities" in this signal are used to trigger the clamp advance circuit.

4.3 The Clamp Advance Circuit

The assumption that adjacent heart cycles tend to be of equal duration is used in the design of the "predictor". By generating a voltage proportional to the duration of a heart period and comparing it with a ramp voltage initiated at the start of the subsequent cycle, one can anticipate the instant of occurrence of the next trigger pulse.

The clamp advance interval can be set by adding a variable bias to the ramp before comparison. Coincidence of the two voltage levels then activates a monostable circuit which closes the clamp relays for 30 milliseconds.

Figure 4.5 is a block diagram of the system and Figure 4.6 is a diagram of the system waveforms. The pulse sequence shown in Figure 4.6a is obtained from the output of the automatic trigger selector, and is used to trigger four monostable flip-flops whose outputs (Figure 4.6b, 4.6c, 4.6d, and 4.6e) control the six gates shown in Figure A.9. As soon as the 0.15-second monostable circuit returns to its stable state, gates numbers one and six open, and capacitors C_1 and C_3 (Figure 4.5) begin to charge, and continue to do so until the next trigger pulse arrives. The capacitors are fed from constant-current sources and the voltages appearing across them therefore increase linearly with time as shown in Figures 4.6f and 4.6h, reaching final values which are proportional to the



Note: Letters a-j refer to waveforms in Figure 4.6.

Figure 4.5 Clamp advance circuit

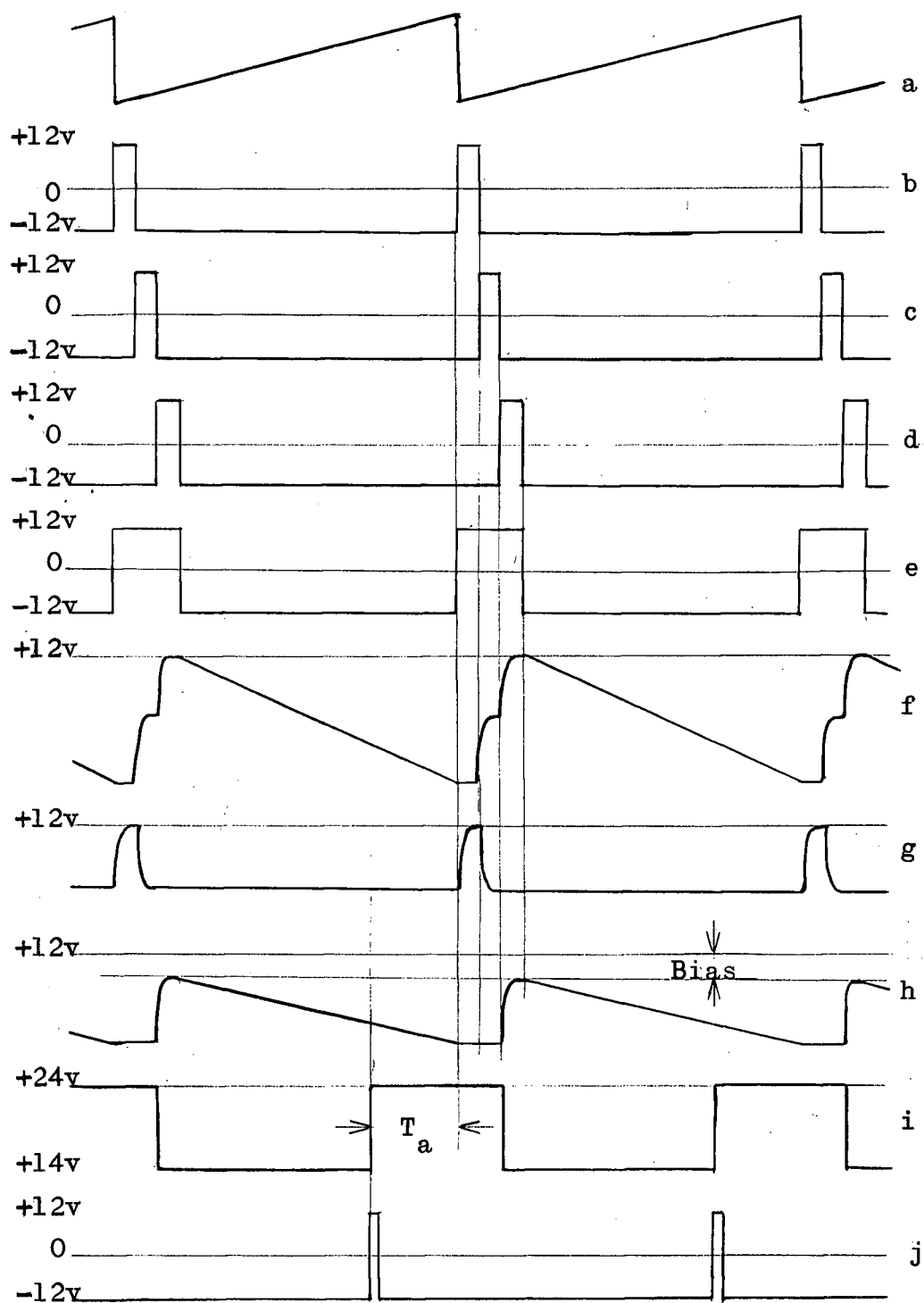


Figure 4.6 Waveforms generated in the clamp advance circuit

period of the heart cycle. Gates two, four, and five reset the capacitors during appropriate intervals in the cycle. When gate number three opens, charge is transferred to the initially-uncharged capacitor C_2 , which then has a voltage one-half that reached on C_1 . This voltage (Figure 4.6g) is compared with the ramp function on capacitor C_3 in the succeeding cycle. A differential amplifier is used for this comparison. The ramp function appearing on C_3 (Figure 4.6h) is biased in order to give the desired clamp advance interval T_a (Figure 4.6i).

5. THE TWO-DIMENSIONAL COMPUTER

5.1 Description

The actual two-dimensional trigonometric computers (Figures 5.1 and A.6) are somewhat different from that described in Chapter 2. The quadrature sinusoids are replaced by quadrature square-waves, that is, square-waves whose fundamental components are in quadrature, and a low-pass filter is inserted between the adder and the detection units. The low-pass filter is designed to pass only the fundamental component of the square-waves and to give a 90° phase-shift at carrier frequency f_0 . This phase-shift is chosen rather than some arbitrary value in order that the phase reference can be made to lie on one of the axes, e.g., the positive x-axis in the frontal computer.

5.2 The Multipliers

Each multiplier used in this device consists of two synchronous gates controlled by square-waves of carrier frequency f_0 . Each gate is made up of a set of complementary transistors connected in the configuration shown in Figure 5.2. The gates are alternately opened and closed by applying the carrier voltages to the bases of the transistors. In the open state, the emitter-base junctions of the transistors are forward-biased putting the transistors into saturation so that the gate has a very low forward resistance, of the order of one ohm. The gates are closed by reverse-biasing the emitter-base junctions. By applying a differential input signal,

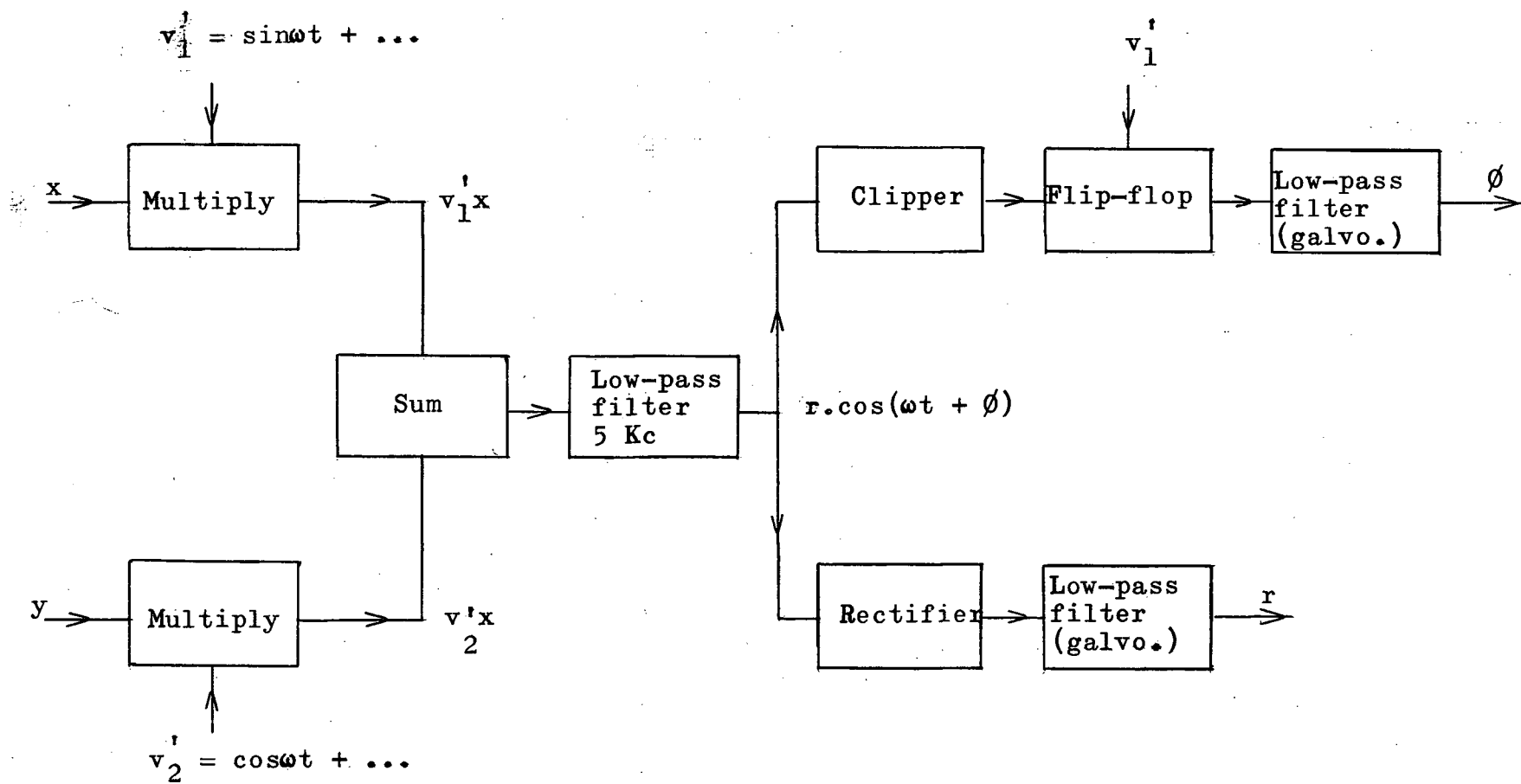


Figure 5.1 Block diagram of the two-dimensional trigonometric computer as constructed

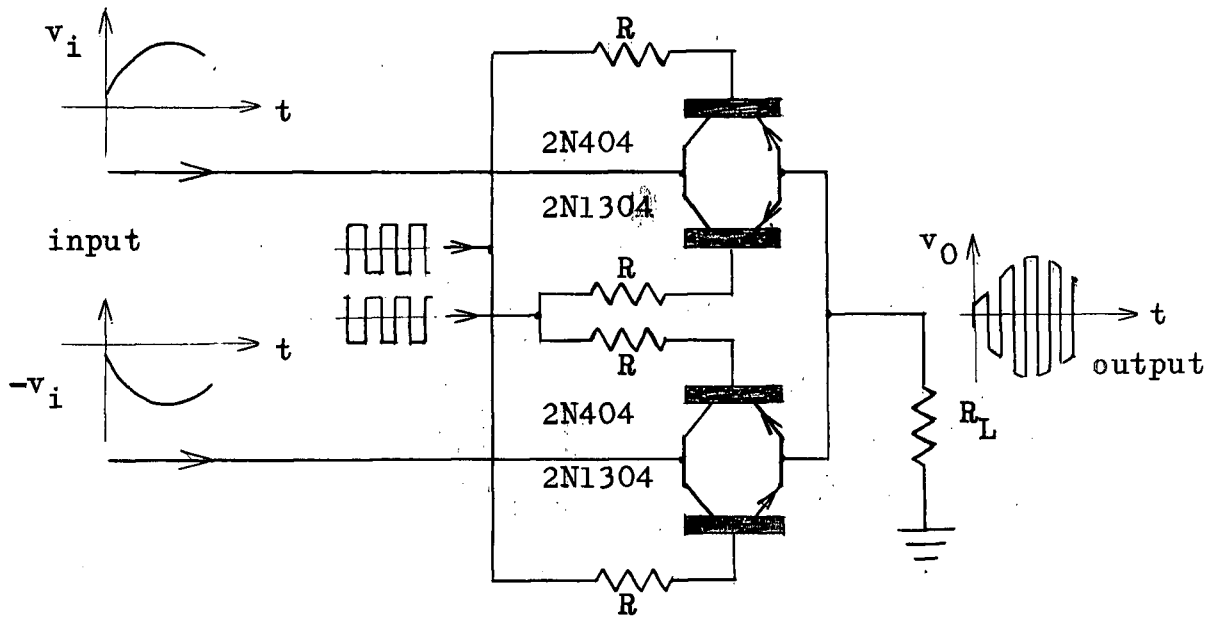


Figure 5.2 Circuit diagram of a multiplier

suppressed-carrier modulation is achieved.

5.3 The Carrier Generator

As in the previous polarcardiograph,⁵ a carrier frequency of four kilocycles per second has been adapted. The gate-type multipliers mentioned above require four square-waves of the type shown in Figure 5.3, which can be obtained as follows. Sixteen-kilocycle clock-pulses are derived from a sixteen-kilocycle astable flip-flop by differentiating and clipping one of its outputs. This pulse sequence is used to trigger a bistable flip-flop (B_1 in Figure 5.4) which gives two eight-kilocycle square-waves 180° out of phase and of equal on-off duration. When these two square-waves are differentiated and clipped, two eight-

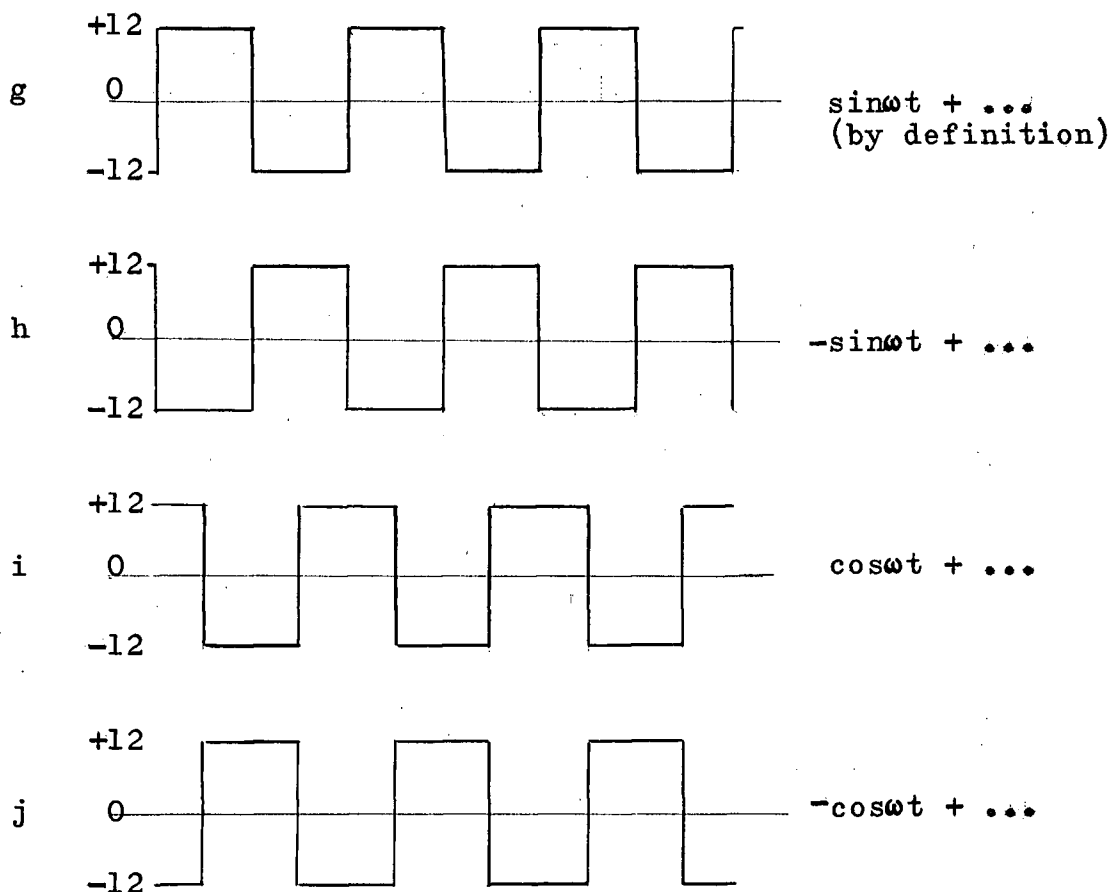


Figure 5.3 Carrier generator output waveforms

kilocycle pulse sequences 180° out of phase are obtained. By using these two pulse sequences to trigger the remaining two bistable flip-flops (B_2 and B_3 in Figure 5.4), there are available at their outputs four four-kilocycle square-waves of equal on-off duration and differing in phase from one another by $n \times 90^\circ$ ($n = 1, 2, 3$).

Note: Letters a-f refer to Figure 5.5.
Letters g-j refer to Figure 5.3.

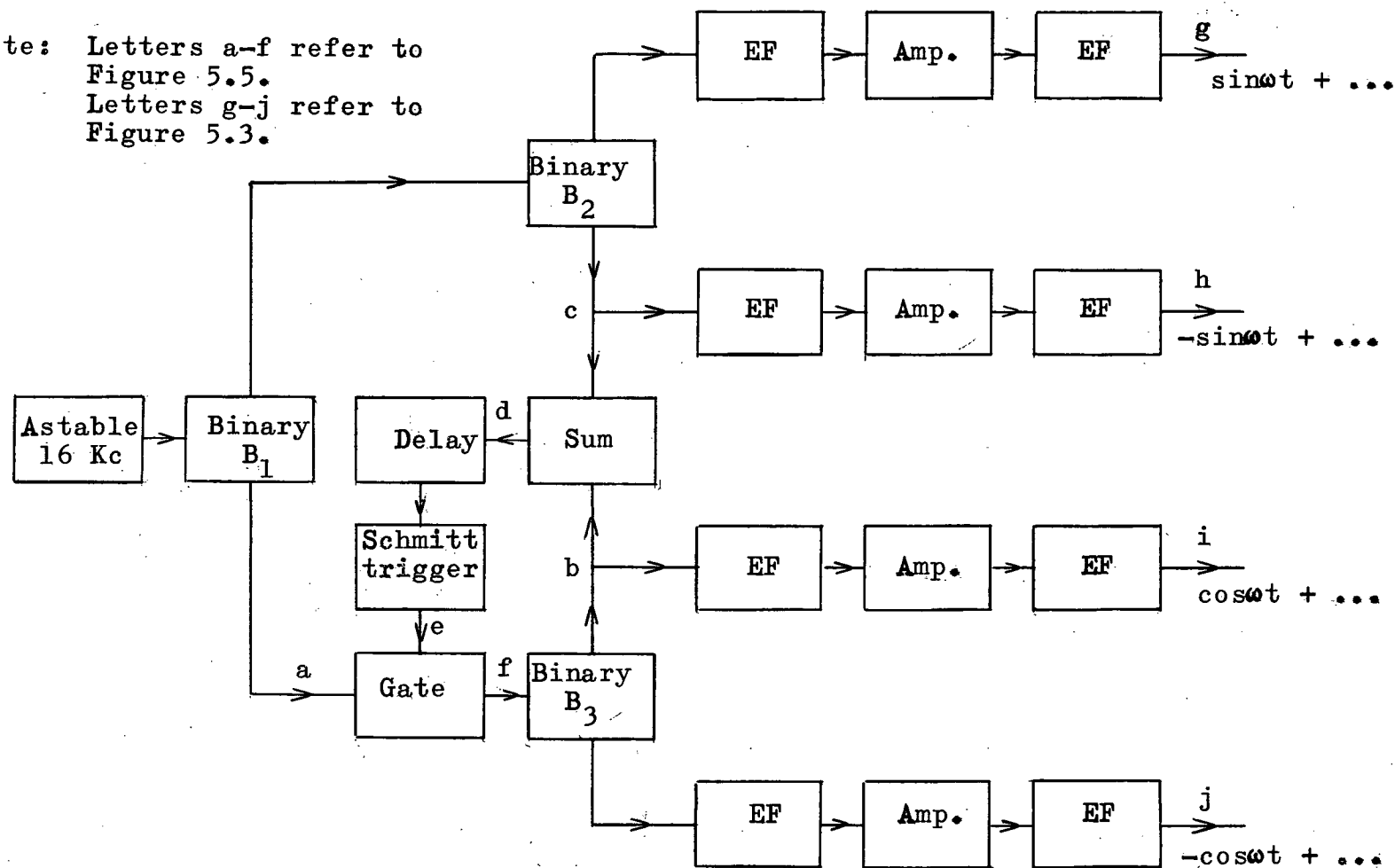


Figure 5.4 4-kc carrier generator

If we say that one of the square-wave outputs of B_2 has a fundamental component equal to $\sin\omega_0 t$, then the other square-wave generated by that bistable unit will have a fundamental component of $-\sin\omega_0 t$. The two remaining four-kilocycle square-waves generated by B_3 will have fundamental components equal to $\cos\omega_0 t$ and $-\cos\omega_0 t$.

In order to establish a fixed phase sequence for the four outputs, independent of the initial states of the bistable units, the pulse train used to trigger B_3 is gated. A gating pulse is obtained by first adding two of the outputs, clipping off the negative portion, and delaying the resultant waveform by τ seconds (Figure 5.5). The delay circuit consists of an RC integrator and a Schmitt trigger (Figure A.7).

The gating circuit works as follows. If the four output waveforms have the proper sequence, a gating pulse (Figure 5.5e) is generated. However, if the desired sequence does not appear, a gating pulse is not generated, thus blocking one of the pulses triggering B_3 , which causes its output to shift by 180° and return to its proper sequence.

Figure A.7 is a complete circuit diagram of the carrier generator. A potentiometer is used in the astable flip-flop in order to adjust the clock frequency. The emitter-follower configuration used in the output circuits was dictated by the magnitude of the output signals (± 12 volts) and the need for low output resistance.

5.4 The Low-pass Filter

The four-kilocycle fundamental component is extracted from the summed multiplier outputs by a low-pass filter

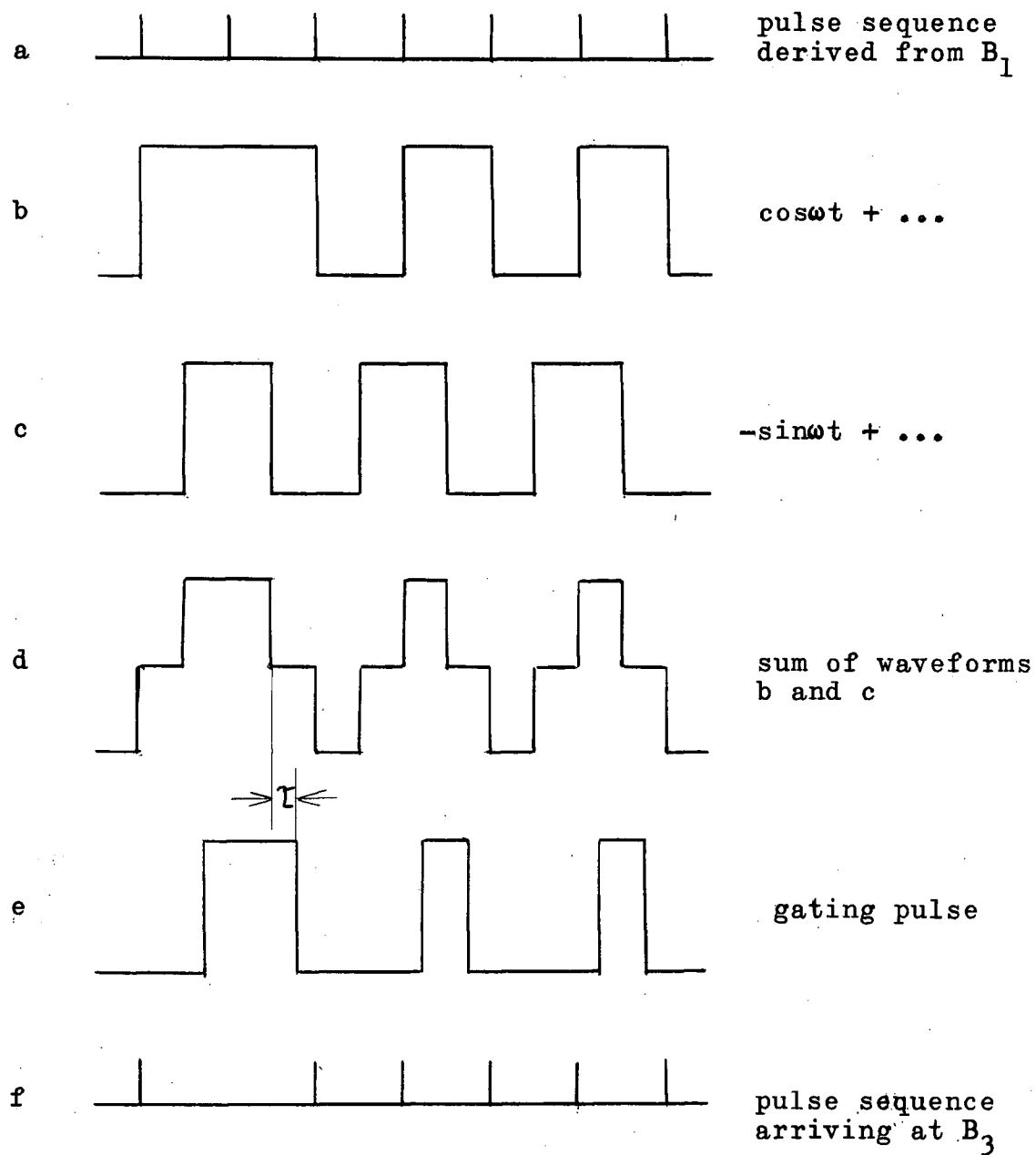


Figure 5.5 Waveforms used to ensure correct phasing of carrier generator outputs

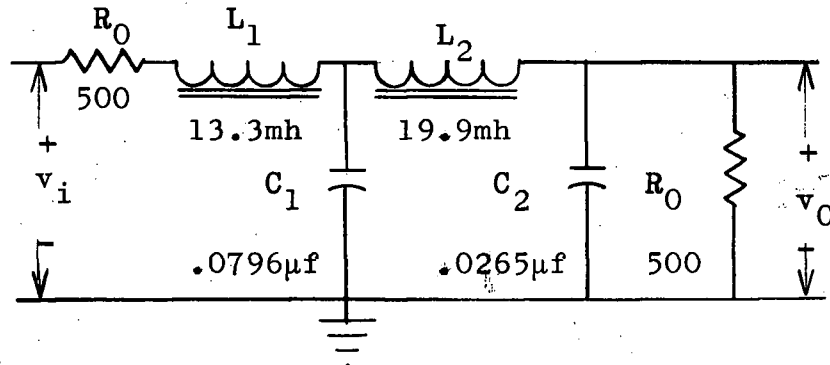


Figure 5.6 Low-pass filter

designed using the insertion-loss technique (Figure 5.6). It produces 90° phase-shift at four kilocycles and 270° phase-shift at twelve kilocycles. The phase-shift at twelve kilocycles was set at some multiple of 90° in order to avoid a resultant phase-shift due to the residual third-harmonic component of the filtered waveforms. Second-harmonic components are absent because the waveforms are the sum of square-waves. The insertion loss at four kilocycles and at dc was made equal to zero. The filter characteristics are shown in Figure 5.7.

5.5 Magnitude Detection

A voltage proportional to the magnitude, r , of the heart vector is obtained from the signal $r \cdot \sin(\omega t + \phi)$ (Figure 5.1) by rectifying and filtering. The filtering is done by the recording galvanometers, and full-wave rectification is accomplished using a complementary transistor configuration (Figure A.7). The low saturation-resistance of the

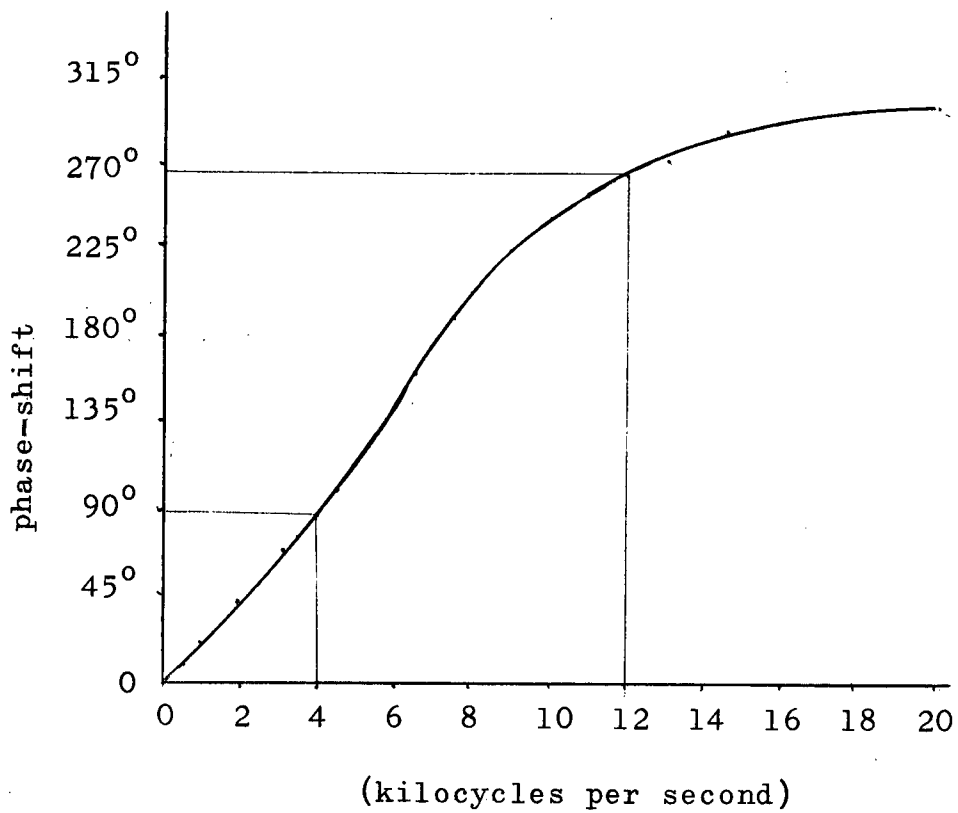
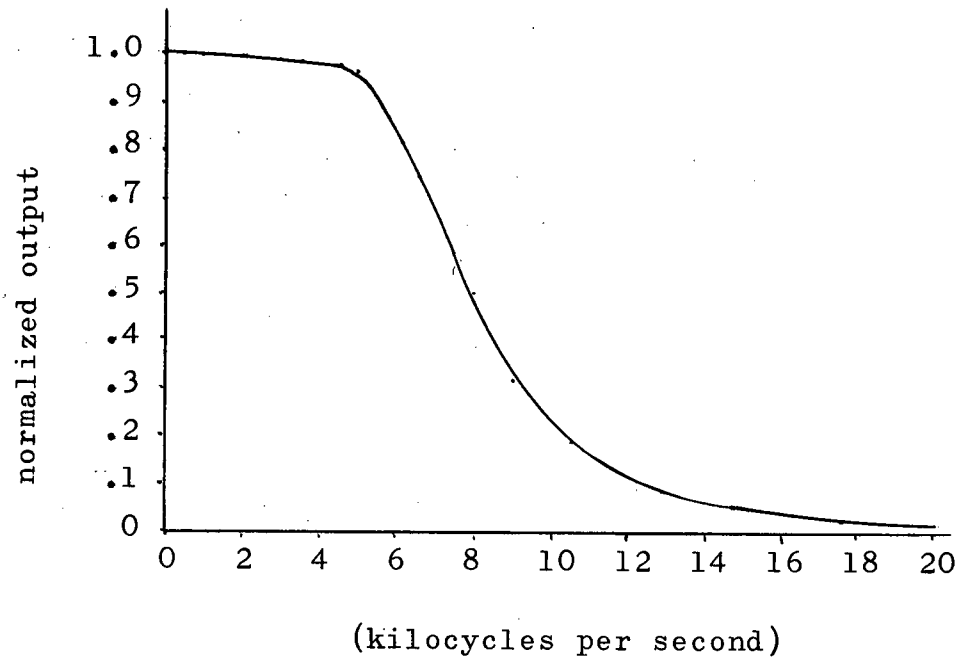


Figure 5.7 Low-pass filter response curves

transistors gives a linear rectifier characteristic over a large voltage range.

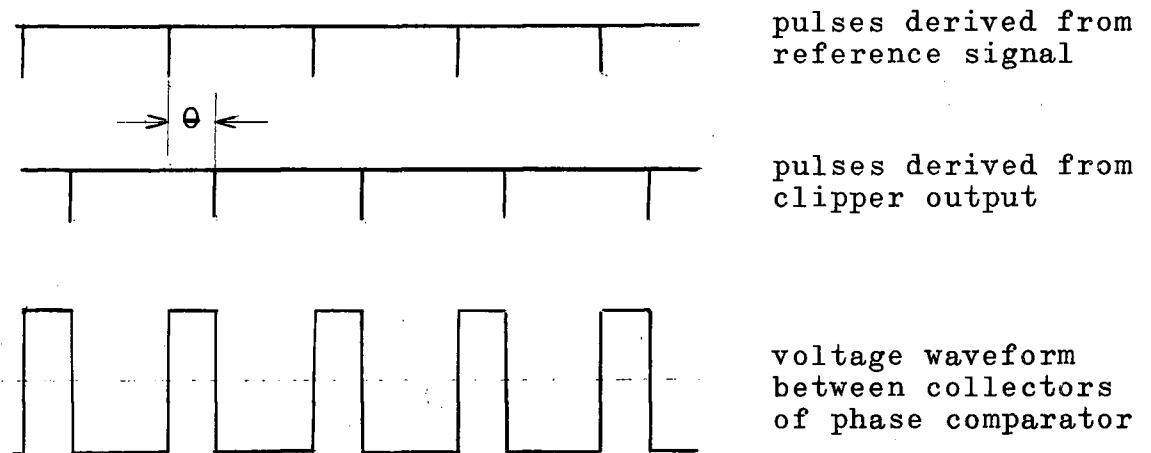


Figure 5.8 Waveform of the phase comparator

5.6 Angle Detection (phase comparison)

Angle detection is carried out in the following manner. The waveform $r \cdot \sin(\omega t + \phi)$ (Figure 5.1) is amplified and clipped in several stages in order to remove the modulation envelope. The resulting square-wave is differentiated and the negative pulses obtained are used to trigger one side of a set-reset bistable flip-flop. The other side of the flip-flop is triggered from corresponding negative

pulses obtained from a square-wave of constant phase, i.e., one of the carrier signals. The average value of the voltage difference between the collectors of the flip-flop is directly proportional to the phase difference, ϕ , between the two pulse sequences triggering it (Figure 5.8). Averaging is accomplished by the recording galvanometers which have a cutoff frequency of 240 cycles per second.

5.7 The Clipper

The clipper has three stages, each consisting of an amplifier, a buffer amplifier (emitter-follower), and a clipping circuit. The first stage has a gain of three and the remaining two stages each have gains of approximately thirty.

The transistor arrangement shown in Figure A.7 is used for clipping the outputs of the first two stages. A forward avalanche voltage of about 0.2 volts across the emitter-base junction of the 2N404 transistor gives this circuit a 0.4 volt peak-to-peak clipped output. The third clipper uses two ordinary diodes and a 6.2-volt zener diode to give a 7-volt peak-to-peak clipped output (Figure A.7). Delays due to transistor saturation are eliminated by having all three amplifiers working in the class-A region.

Each clipper unit has a dynamic range of about 100:1, that is, the clipper will produce a square-wave from magnitudes as low as one percent of maximum signal value.

5.8 The Threshold Circuit

In the signal $r \cdot \sin(\omega t + \phi)$ (Figure 5.1), phase determinations lose significance when r becomes very small because the angle output ϕ becomes very irregular due to noise.

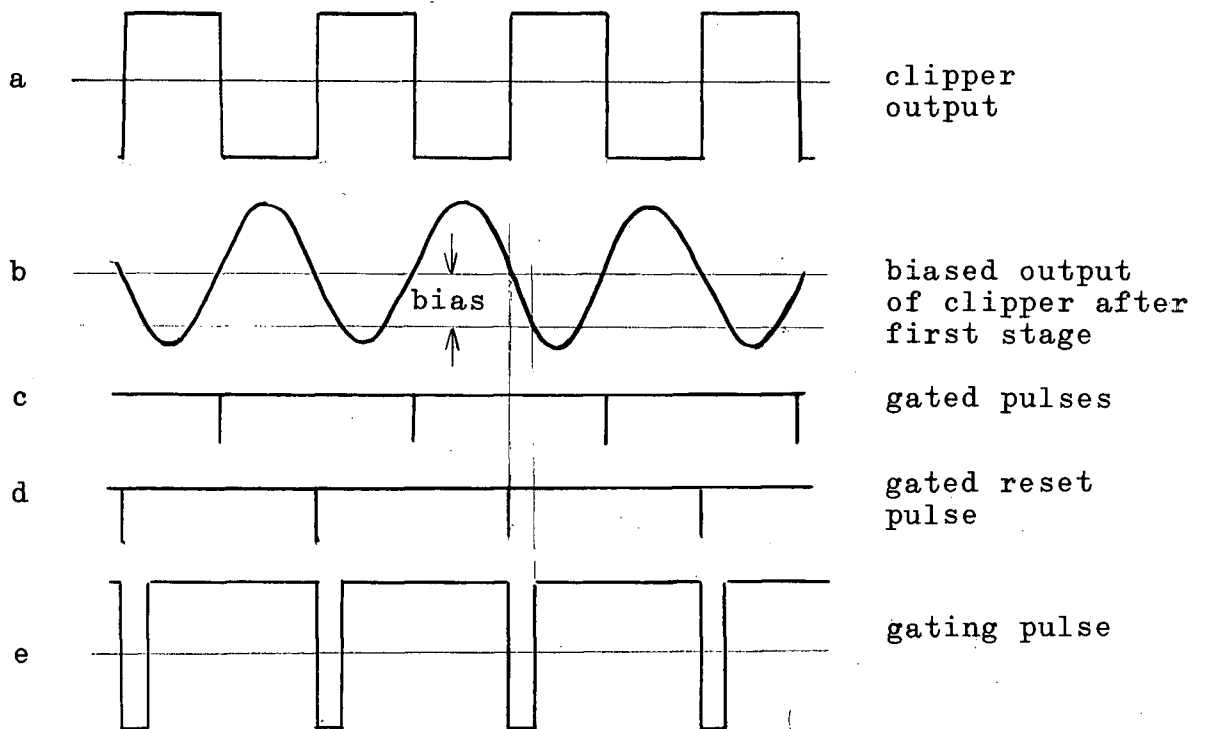


Figure 5.9 Waveforms of threshold circuit

For this reason, the output of the phase detector is set to some predetermined value when the magnitude of the input signals to the computer fall below a value determined by the threshold circuit. The threshold level is adjustable by the operator, and can be varied according to the amount of noise

(muscle tremor, 60-cycle pick-up, etc.) present in the input signals.

The clipped signal derived from $r \cdot \sin(\omega t + \phi)$ is differentiated and enters the phase comparator through a gate which is opened by a signal derived from a set-reset binary flip-flop (Figure 5.10). The gate-opening binary is set by the partially clipped $r \cdot \sin(\omega t + \phi)$ which is biased by the threshold control. It is reset by a pulse sequence 180° out of phase with the signal passing through the gate. The threshold circuit is adjustable so as to inhibit angle outputs over a range from zero to 10 percent of maximum magnitude output level.

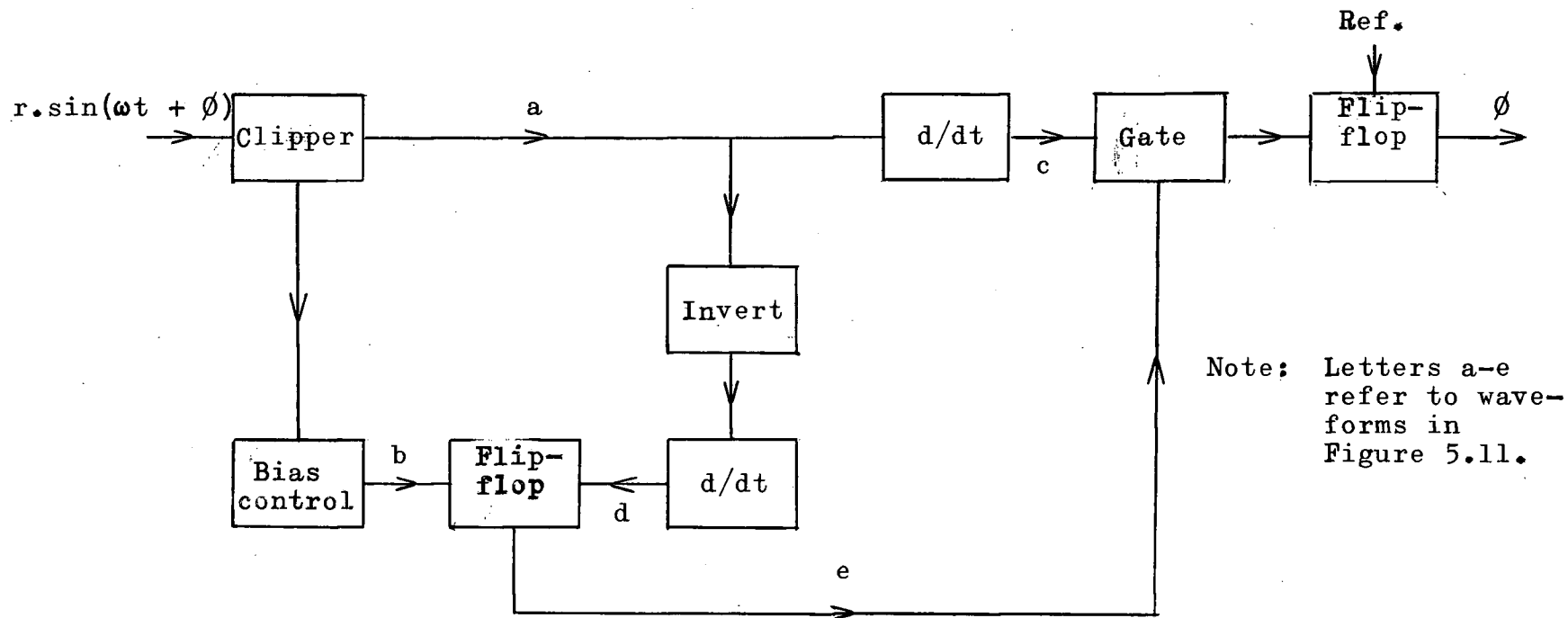


Figure 5.10 Block diagram showing the threshold control circuit

6. THE THREE-DIMENSIONAL COMPUTER

As outlined in Chapter 2, the three-dimensional polar-cardiograph is constructed from a frontal and a polar two-dimensional polarcardiograph of the type described in Chapter 5.

Before the output of the frontal computer (frontal magnitude) can be fed into the polar computer, it must be rectified, filtered, and amplified (Figure 6.1). Rectification is carried out using transistors (Figure A.9) rather than diodes in order to achieve linearity over a large voltage range.

Because the polar angle varies only over 180° , the sudden change in the angle output which occurs in the frontal angle output (zero and 360°) can be avoided by the proper choice of reference signal.

The low-pass filter used for smoothing the rectified output from the frontal computer is of the same design as that described in Chapter 5, except that it is scaled to give a cut-off of approximately 500 cycles per second rather than five kilocycles per second. Because of its low cut-off frequency, this filter introduces an appreciable time delay (approximately 700 microseconds) which is compensated for by the insertion of a similar filter at the z input to the polar computer. Although this 700-microsecond delay occurs in the magnitude and angle outputs of the polar computer, it is insignificant when the time-scale of the recordings is taken into account.

Simultaneous recordings of the spherical coordinates using three different choices of the polar axis is accomplished by using three of the above three-dimensional computers.

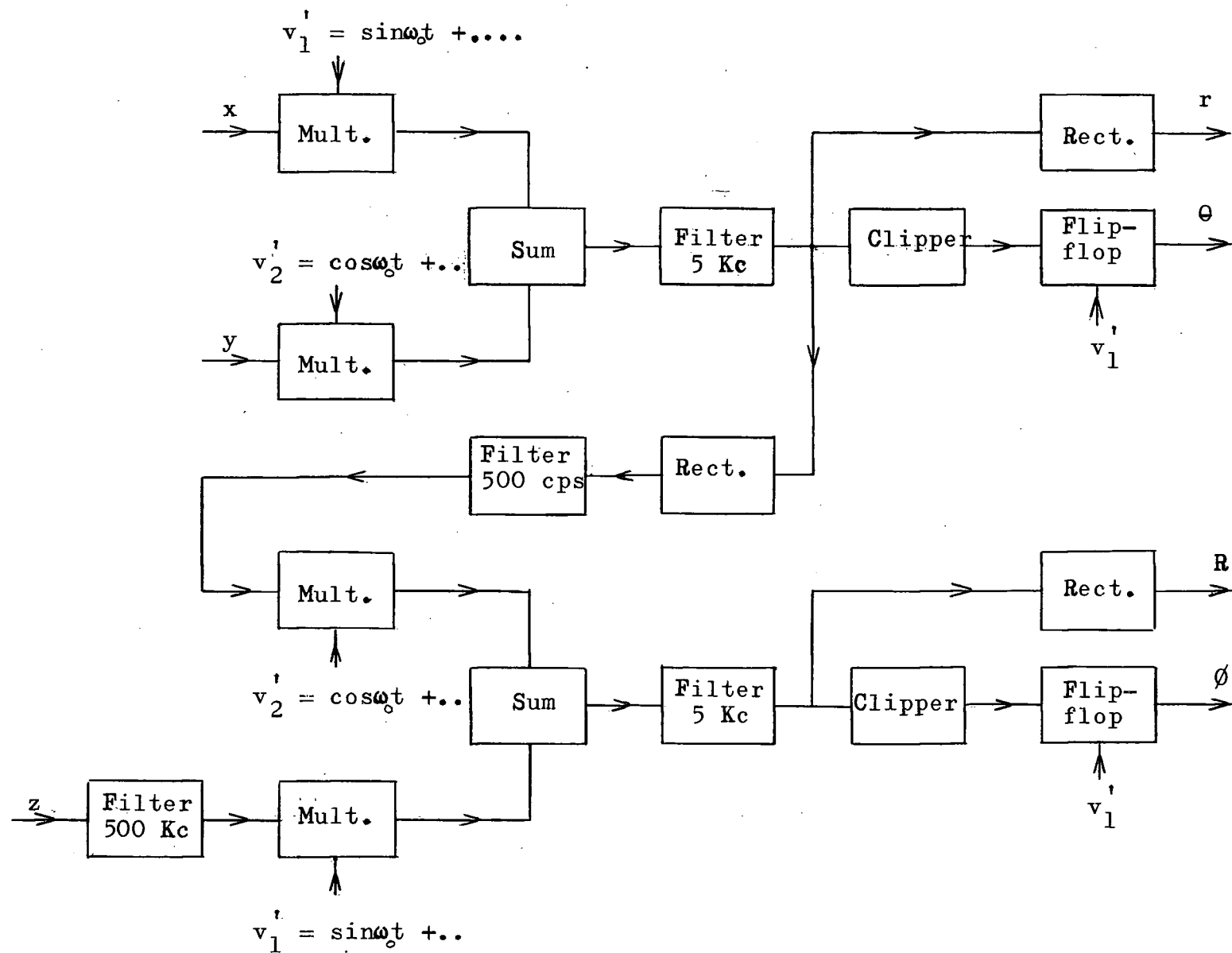


Figure 6.1 Block diagram of the three-dimensional polarcardiograph

7. TEST RESULTS

The linearity of the magnitude outputs of the two and three-dimensional computers was demonstrated by applying test signals at 20 cycles per second to their inputs and measuring the detected output signals as displayed by a Honeywell Type 1508 Visicorder. The input voltages were measured by observing the peak-to-peak signals as displayed on a CRT.

The overall angular response of these two computers was demonstrated by applying equal-amplitude sine and cosine signals at 1 cycle per second to their inputs. Since the vector locus of such a set of signals is a circle whose centre is at the origin, the angle output for the two-dimensional device should be a sawtooth waveform. Because the output of the frontal computer is always a positive quantity, the polar-angle output of the three-dimensional computer should be a triangular waveform.

The operation of the threshold circuit was demonstrated by joining together the inputs of the two-dimensional computer and applying a sinusoid of about 25% maximum amplitude at 1 cycle per second. Because the signal feeding both inputs is the same, its angle output should be a square-wave function which switches between $+45^{\circ}$ and -135° while the magnitude output should be a rectified sine wave. By varying the threshold level, the angle output was made to switch to the reference level of $+180^{\circ}$ for that portion of the cycle for which the magnitude of the input signal was below the threshold level.

The threshold level is indicated as a percentage of the maximum signal level (e.g., a threshold level of 3% corresponds to an equivalent input signal of 0.45 volts peak-to-peak).

The results of the above tests are shown in Figures 7.1 to 7.5.

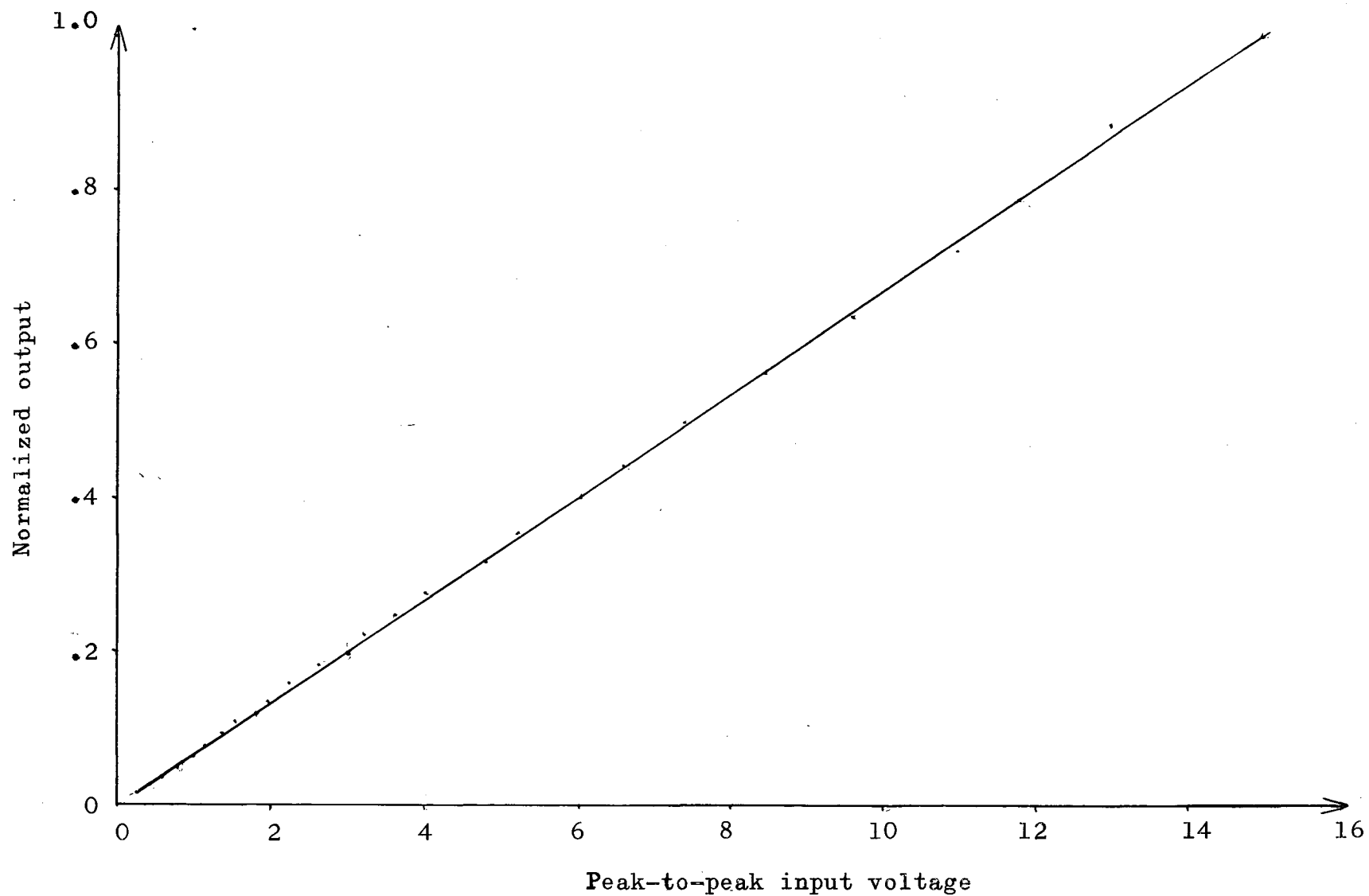


Figure 7.1 Plot of detected output as a function of input for the two-dimensional computer

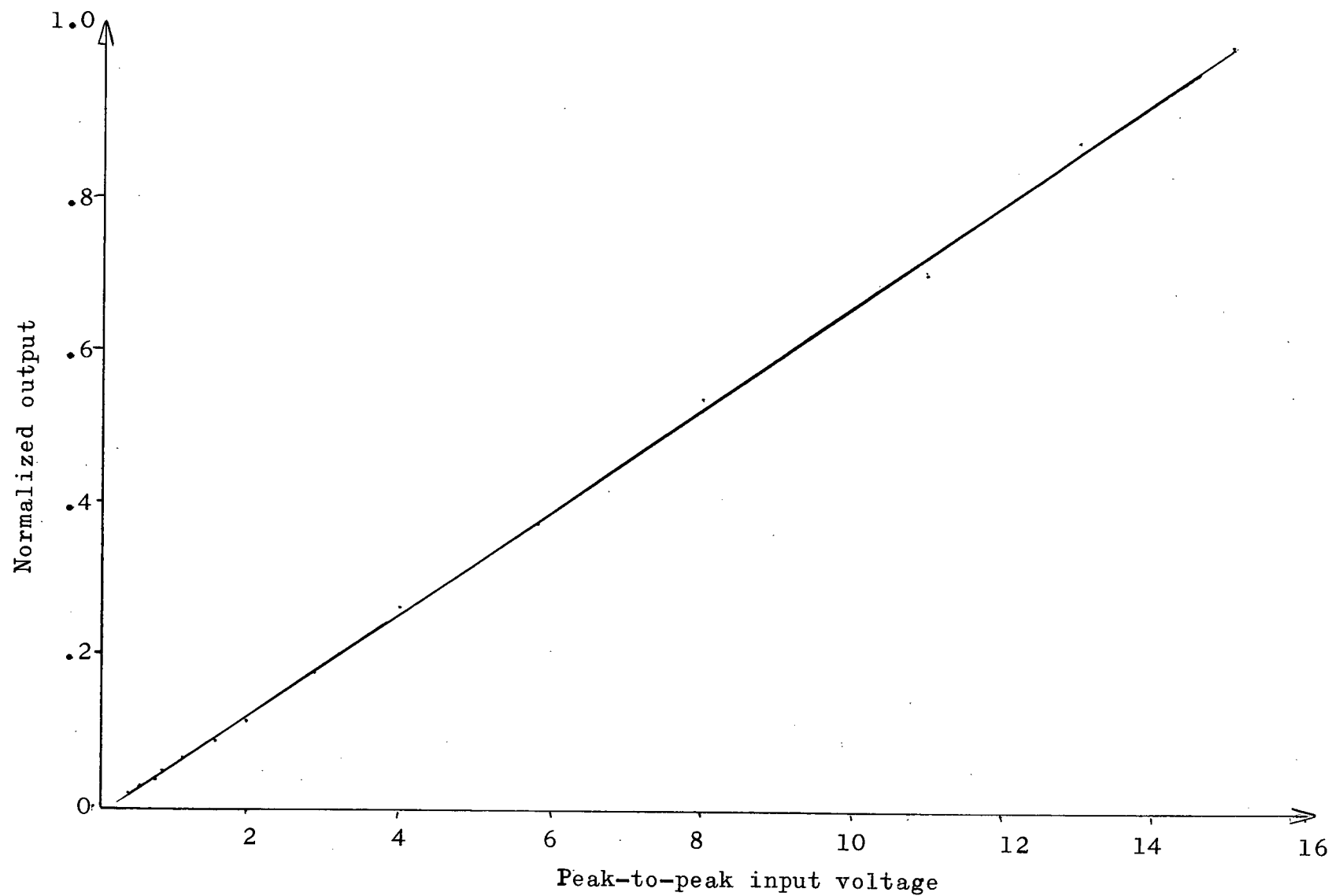


Figure 7.2 Plot of detected output as a function of input for the three-dimensional computer

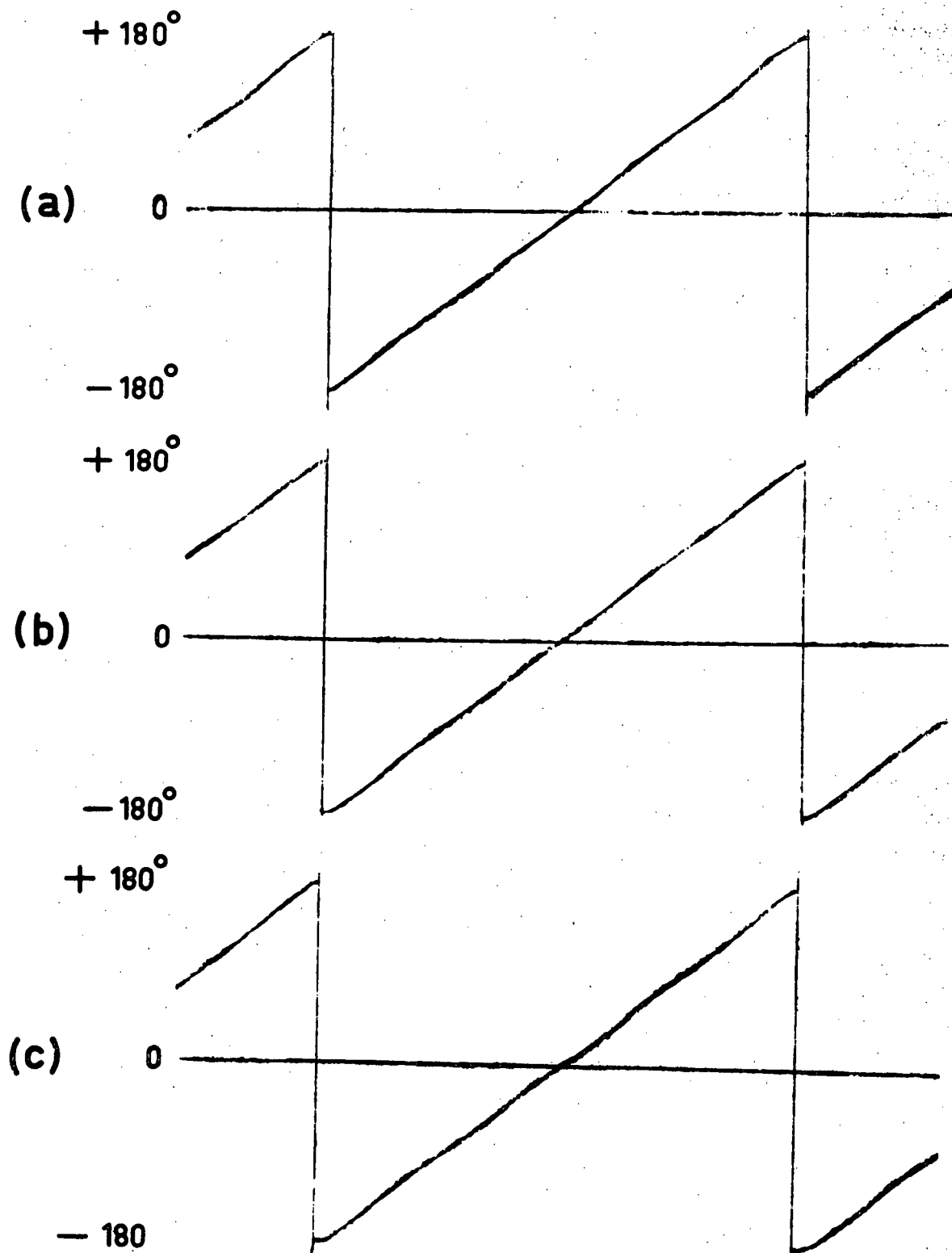


Figure 7.3 Recording of angle outputs of the two-dimensional computer for three different peak-to-peak input-signal levels, (a) 15 volts, (b) 4 volts, (c) 0.8 volts

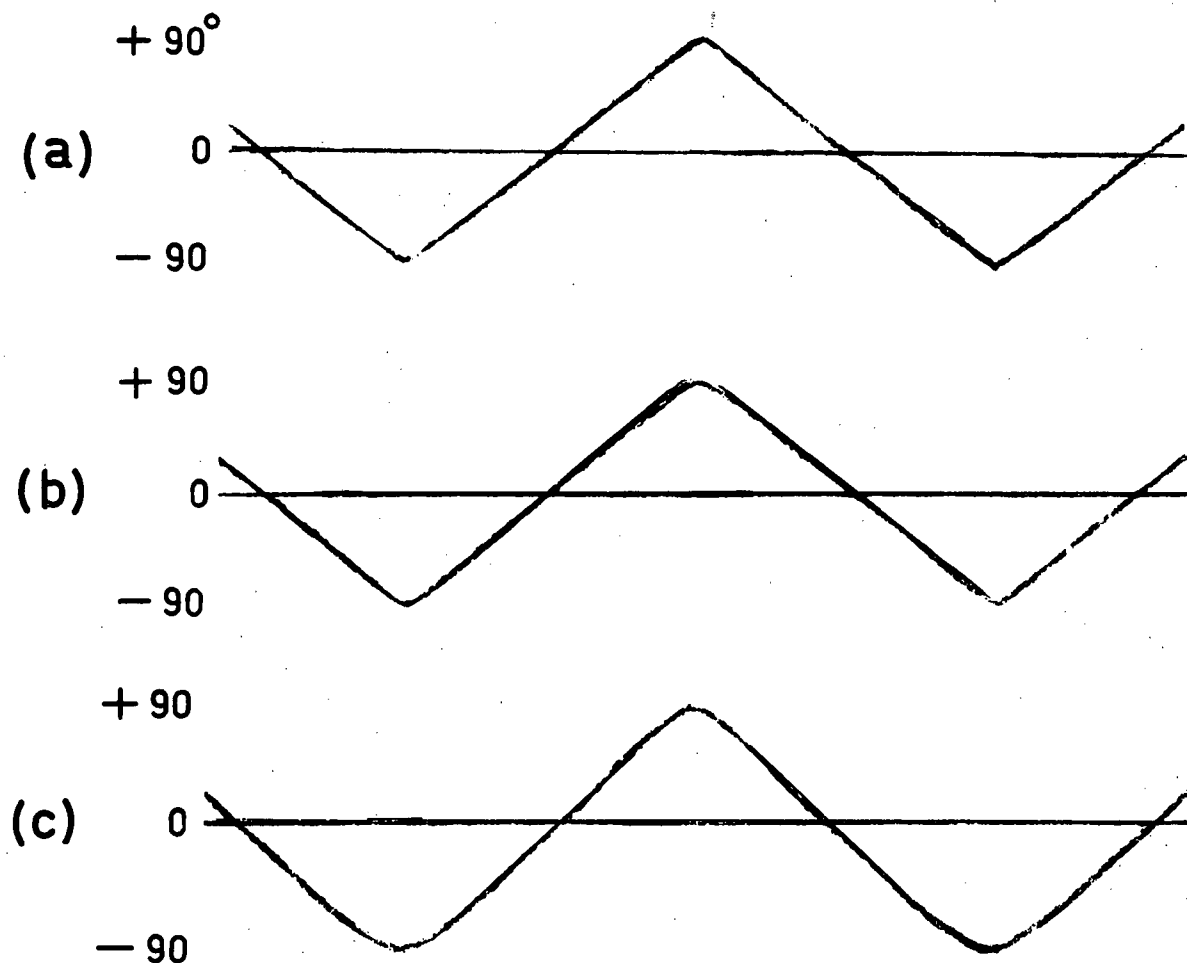


Figure 7.4 Recording of polar angle output of the three-dimensional computer for three different peak-to-peak input-signal levels, (a) 15 volts, (b) 4 volts, (c) 0.8 volts

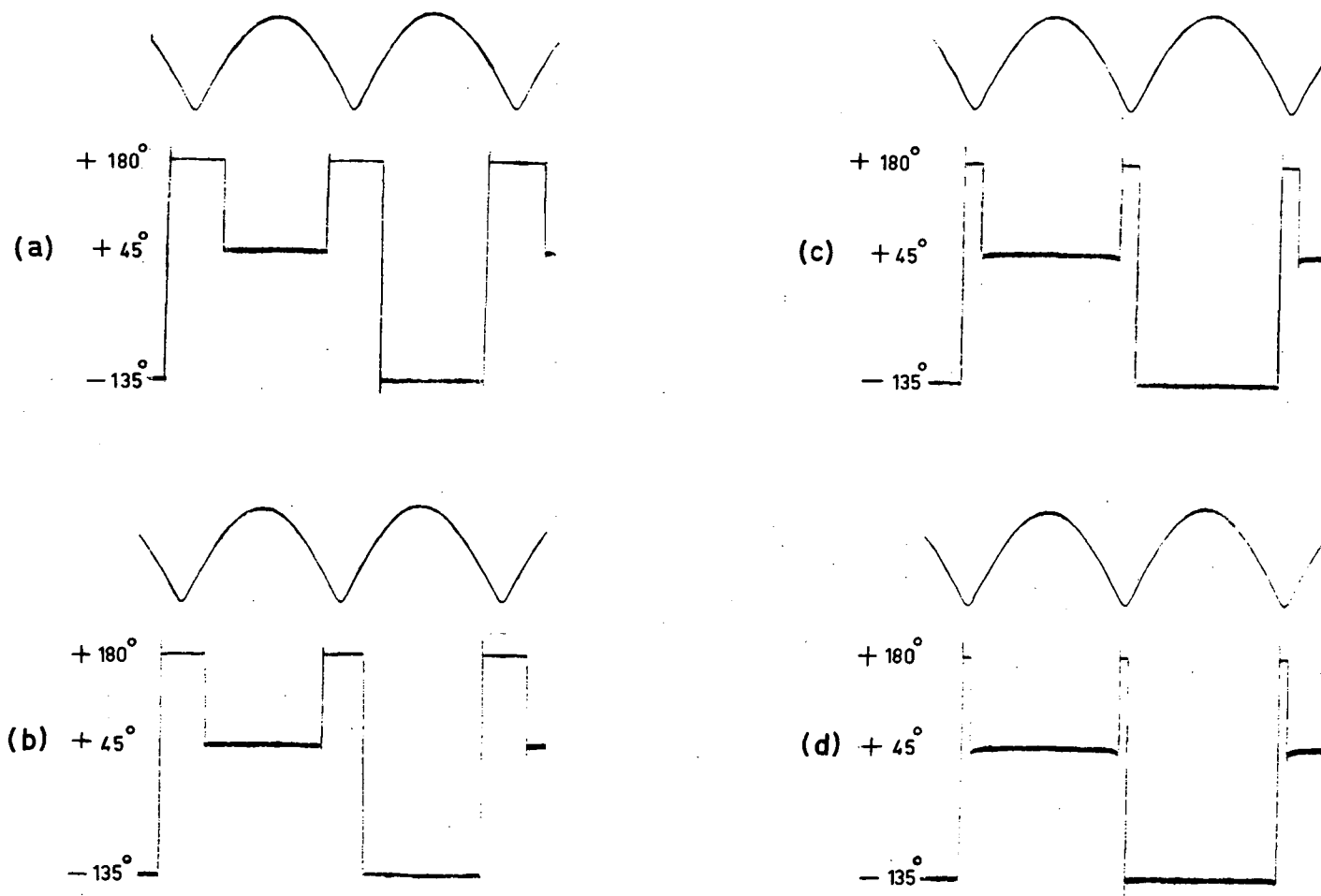


Figure 7.5 Recording of angle output of the two-dimensional computer showing threshold circuit in operation for four different threshold levels, (a) 10%, (b) 7%, (c) 3%, (d) 1.5%

8. CONCLUSIONS

The design of a two-dimensional polarcardiograph and the use of two such two-dimensional devices to realize a three-dimensional polarcardiograph has been described, together with the circuitry necessary to derive and amplify a set of voltages proportional to the Cartesian coordinates x , y , and z .

Although the instrument has not yet been tested clinically, tests performed on it in the laboratory indicate that it is well within the accuracy required. Both the frontal and polar magnitude outputs were shown to remain linear even for small input signals. When tested with signals of the order of 5% of maximum input signal level, the frontal angle output maintained its calibration, while the polar angle output started to show slight distortion.

The base-line clamping system, including the automatic trigger selector and the clamp advance circuit, was tested using a simulated heart waveform and found to function satisfactorily.

APPENDIX

The three-dimensional computer described in this thesis has been subdivided into ten different sections and assembled on printed circuit boards. Each printed circuit card is six by nine inches in size and is designed to plug into a standard 22-pin Amphenol connector. The letters in the following circuit diagrams, Figures A.1-10, correspond to the terminal lettering of the Amphenol connectors.

A brief description of each printed circuit card (P.C.C.) type follows:

P.C.C. #1.

The seven preamplifiers described in Chapter 3 and shown in Figure A.1 are assembled on this unit.

The potentiometer R_5 is for centring. The input terminal marked Z is common to all seven amplifiers and is used as a patient ground. Each amplifier is decoupled from the +24 and -24 volt supplies.

P.C.C. #2.

The three second-stage amplifiers and the third-stage emitter-follower outputs associated with each are assembled in this unit. A description of these amplifiers is given in Chapter 3 and the circuit diagram is presented in Figure A.2.

Centring is obtained by adjustment of R_{10} . A variation in gain of about 20% is available by adjusting R_{19} . R_{20} is used to set the output level to zero volts. Each of the units shown in Figure A.2 is decoupled from the +24 and -24 volt power supplies.

P.C.C. #3.

The Frank and RAFE lead-system networks described in Chapter 3 and shown in Figure A.3 are mounted on this unit.

Provision is made in the printed circuit layout so that emitter-followers may be inserted at the inputs to the networks. All printed circuit connections are made on one side of the unit while the reverse side is kept intact so that it serves as a shield.

P.C.C. #4.

The coupling capacitors and feedback circuitry (relays, etc.) described in Chapter 4 are mounted on this card.

P.C.C. #5.

The automatic trigger selector, the clamp delay circuit, and the relay trigger circuit (Chapter 4) are assembled on this printed circuit card. The circuit diagram for these units is shown in Figure A.5.

The clamp delay time is set by adjustment of potentiometer R_{19} .

P.C.C. #6.

The clamp advance circuit shown in Figure A.6 and described in Chapter 4 is assembled on the printed circuit card.

The slope of the ramp function shown in Figure 4.6h is controlled by R_{43} . R_{60} is used to adjust the clamp advance time; it is actually located on the control panel and connected to the card through terminals P, R and S.

P.C.C. #7.

The complete circuit of the two-dimensional computer described in Chapter 5 and shown in Figure A.7 is assembled on this unit.

The inputs to the computer are equalized by adjustment of R_{10} . Potentiometers R_{44} and R_{52} control the amplitude of the magnitude and angle outputs respectively.

P.C.C. #8.

The circuitry for the carrier generator (Figure A.8) described in Chapter 5 is assembled on this unit.

Potentiometer R_2 is adjusted to give the required four-kilocycle output frequency.

P.C.C. #9.

Three of the threshold units (Figure A.8) described in Chapter 5 are assembled on one printed circuit card.

P.C.C. #10.

This unit contains the circuitry shown in Figure A.10 and described in Chapter 6, necessary for obtaining the third coordinate.

Potentiometers R_{19} and R_{35} are used for centring, while R_{25} is a gain adjustment.

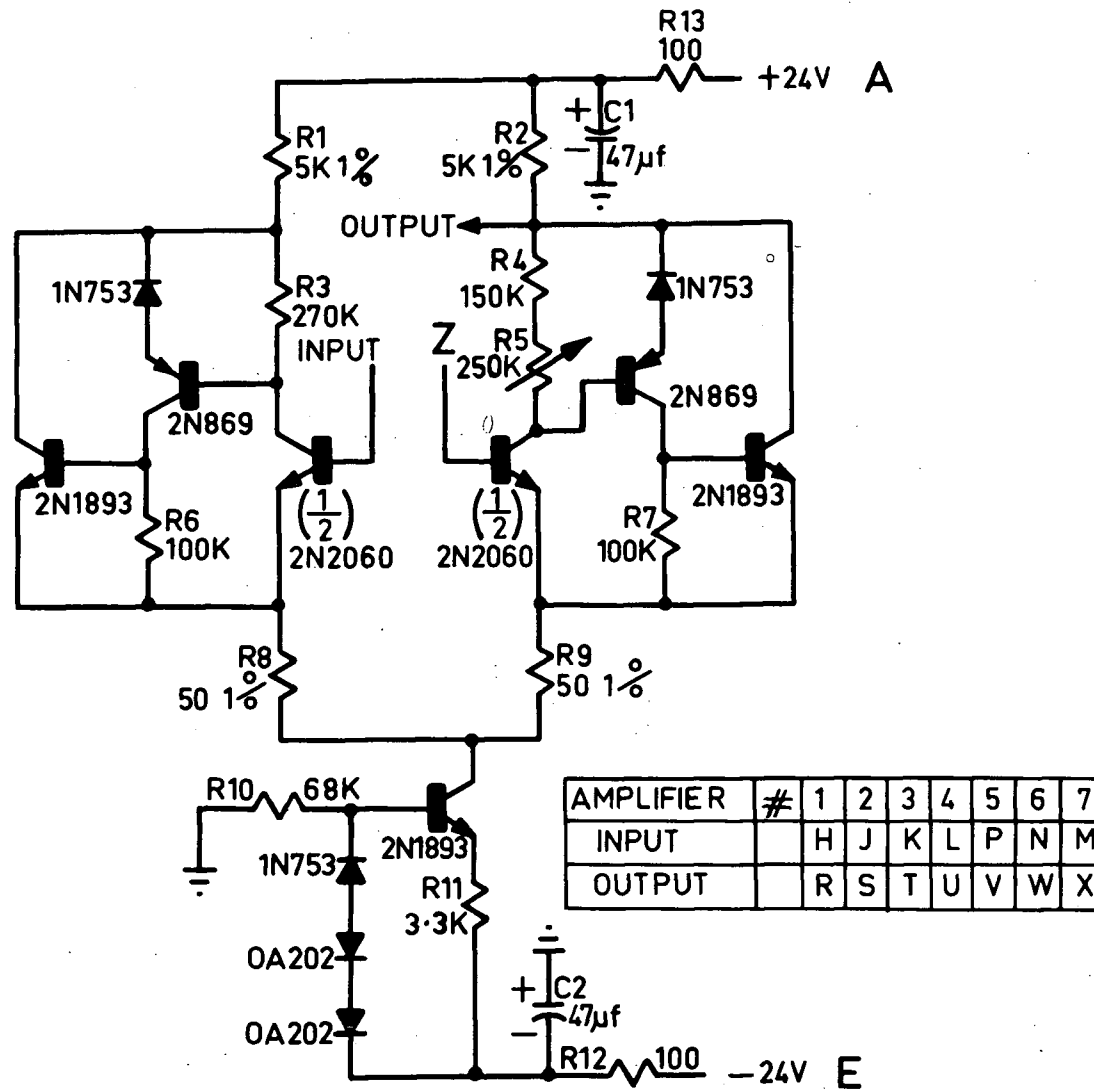


Figure A-1 Circuit Diagram for Preamplifiers



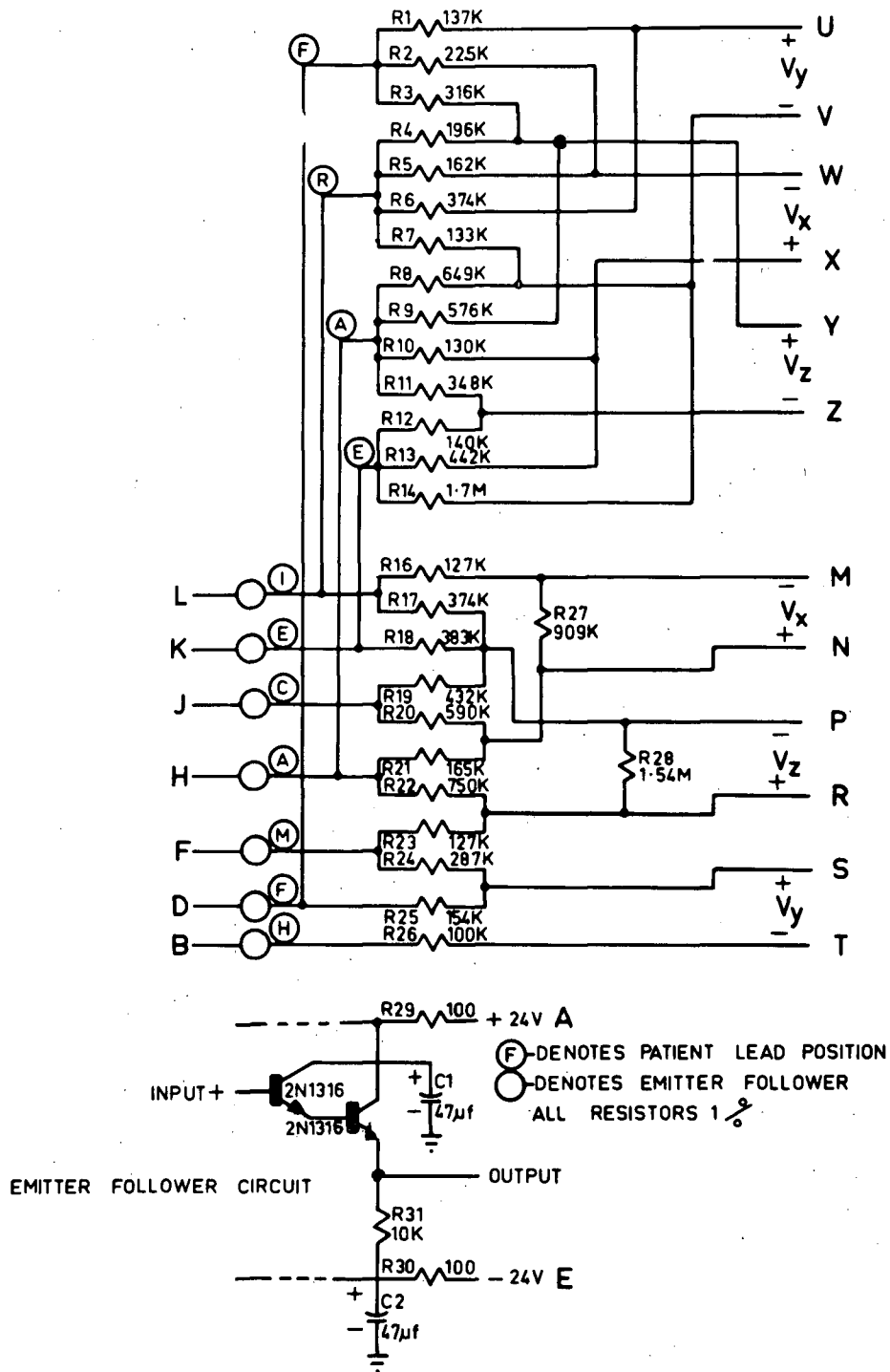
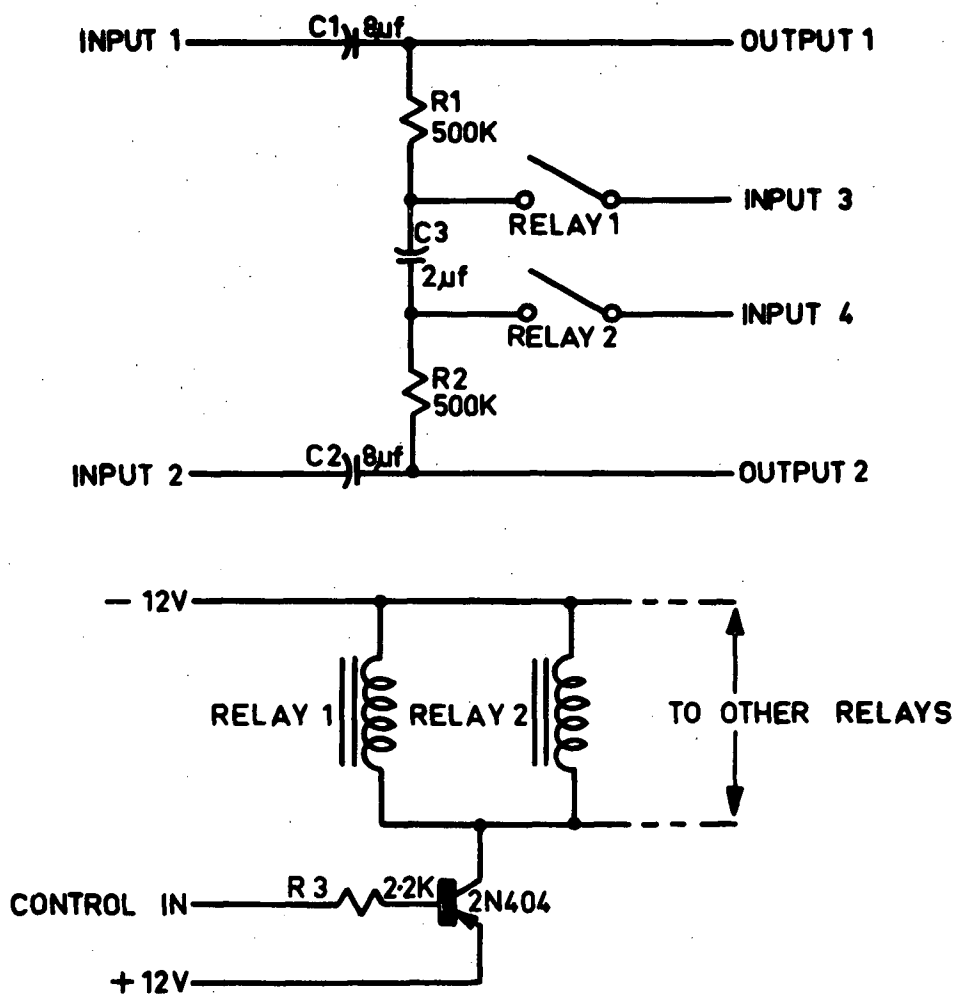


Figure A-3 Circuit Diagram for Frank and RAFE Lead Systems



	INPUT 1	INPUT 2	INPUT 3	INPUT 4	OUTPUT 1	OUTPUT 2
CIRCUIT 1	W	V	A	F	M	N
CIRCUIT 2	U	Z	H	J	P	R
CIRCUIT 3	Y	X	K	L	S	T

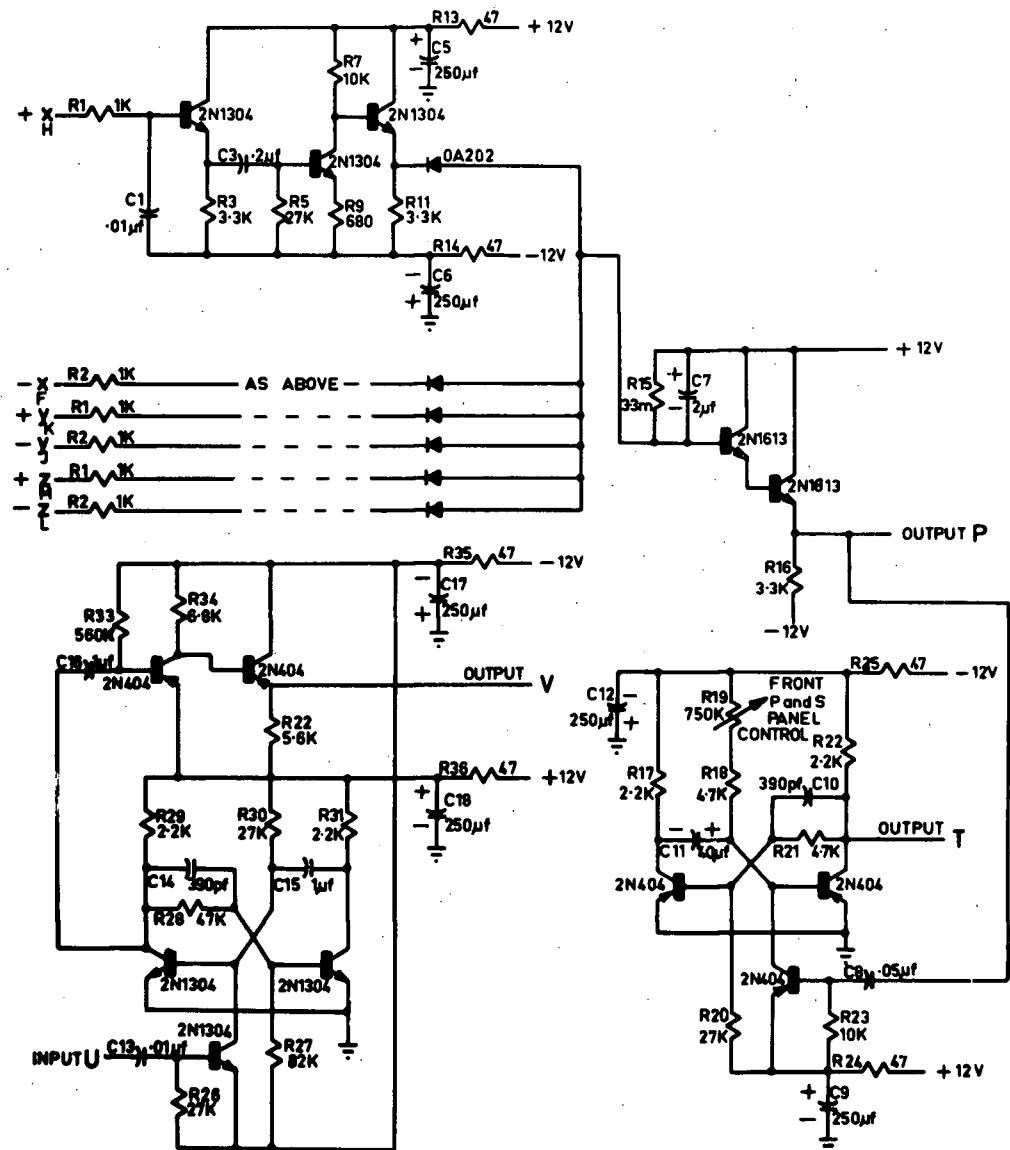


Figure A-5 Circuit Diagram for Automatic Trigger Selector

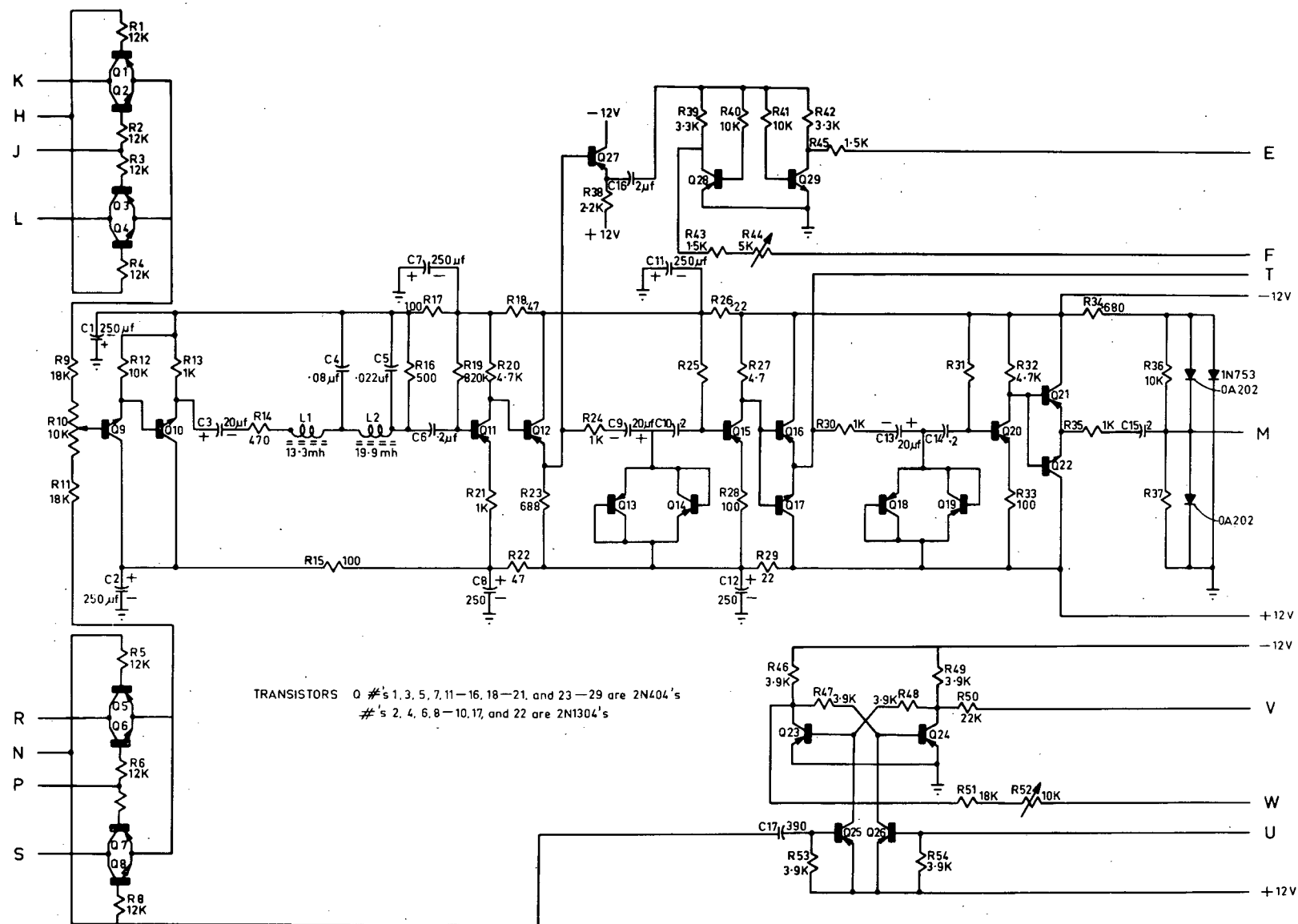


Figure A-7 Circuit Diagram for Two-dimensional Computer

TRANSISTORS Q #'s 1-25 are 2N404's
's 26-29 are 2N1304's

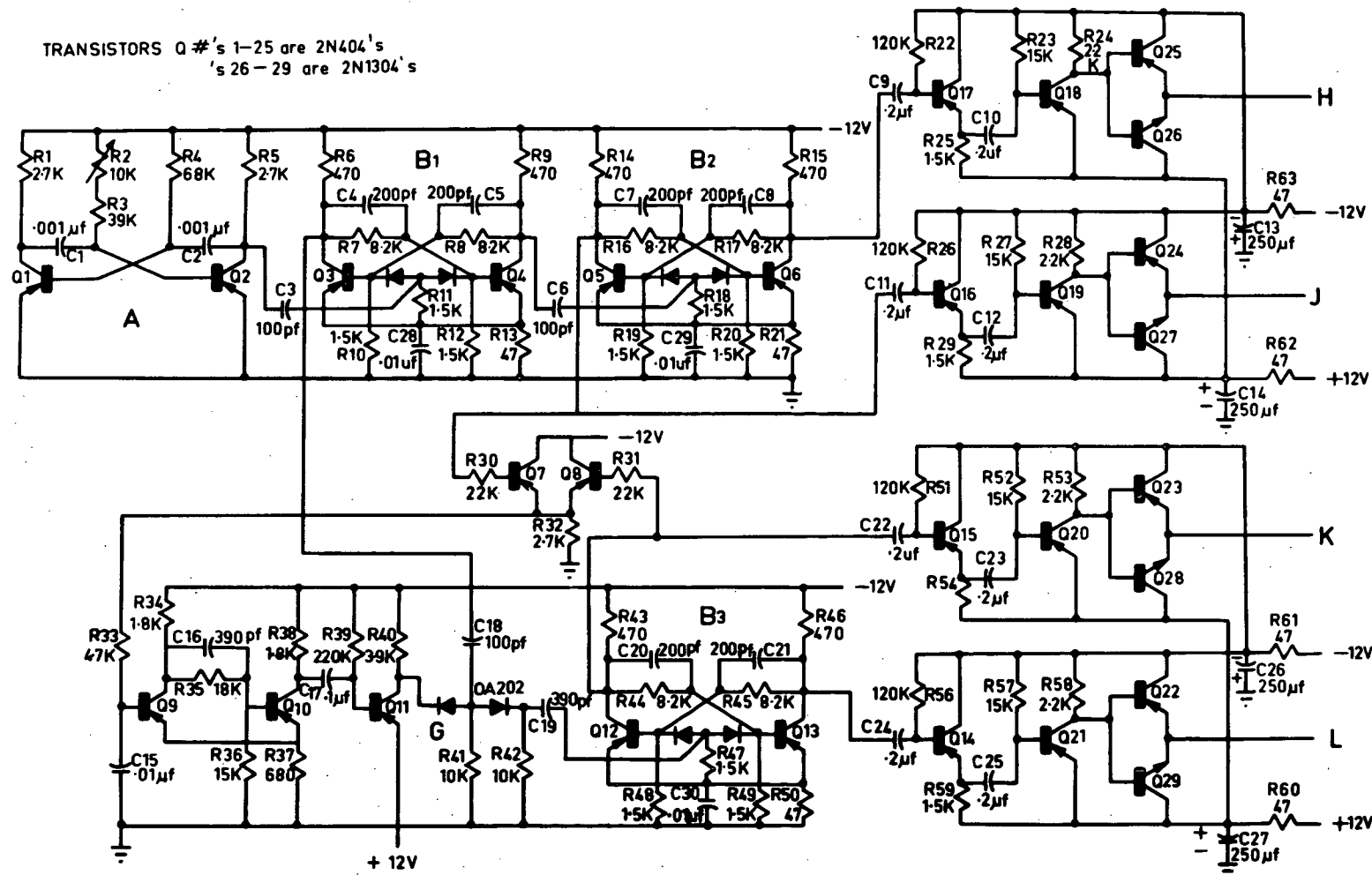


Figure A-8 Circuit Diagram for 4KC Carrier Generator

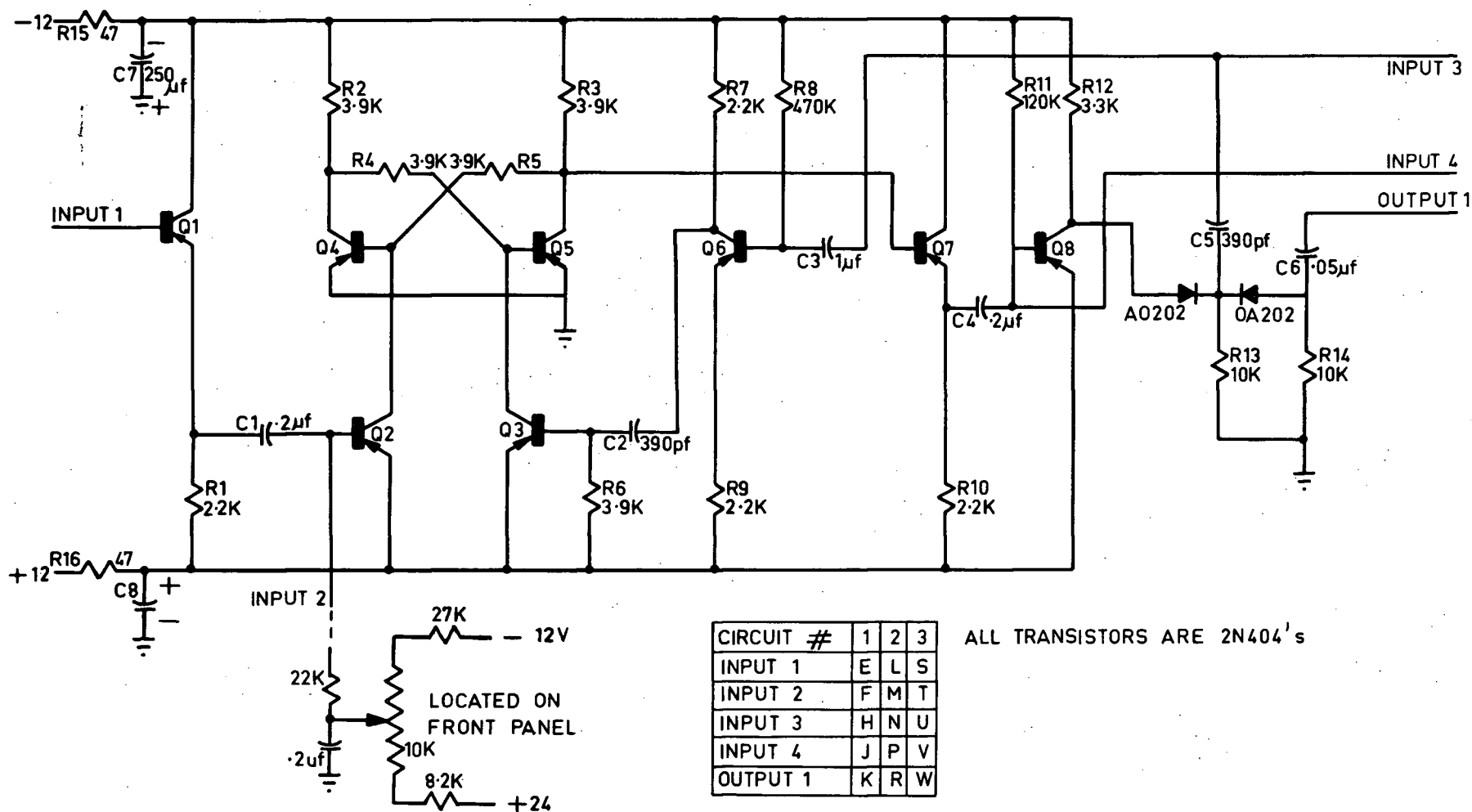


Figure A-9 Circuit Diagram for Threshold Control

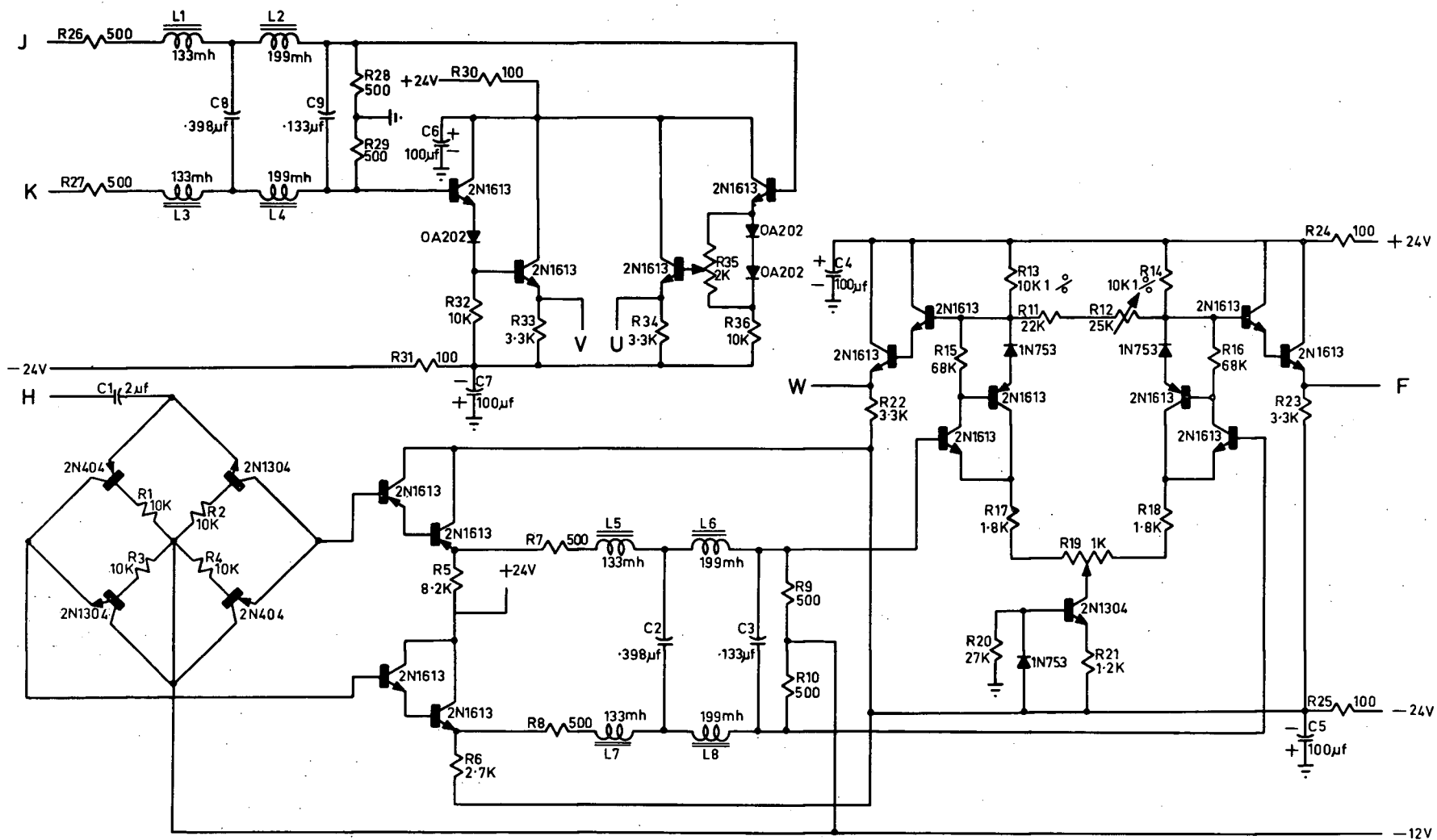


Figure A:10 Circuit Diagram for Frontal Magnitude Detector
and Polar Axis Delay

REFERENCES

1. Einthoven, W., Fahr, G. and de Waart, A., "On the Direction and Manifest Size of the Variations of Potential in the Human Heart and on the Influence of the Position of the Heart on the Form of the Electrocardiogram", translated by Hoff, H.E. and Sekelj, P., Am. Heart J., 40:163, (1950).
2. Canfield, R., "On the Electrical Field Surrounding Doublets and its Significance from the Standpoint of Einthoven's Equations", Heart (New York, N.Y.), 14:102, (1927).
3. Frank, E., "The Elements of Electrocardiographic Theory", Trans. AIEE (Communications and Electronics), p. 125, (May, 1953).
4. Glasset, O., "Medical Physics", The Year Book Publishers Inc., Chicago, Ill., p. 241, (1960).
5. Moore, A.D., Harding, P. and Dower, G.E., "The Polarcardiograph. An Analogue Computer that Provides Spherical Polar Coordinates of the Heart Vector", Am. Heart J., 64:382-391, (September, 1962).
6. McFee, R., "A Trigonometric Computer with Electrocardiographic Applications", Rev. Sc. Instr., 21:1031, (1950).
7. Sayers, B.McA., "A Spatial Magnitude Electrocardiograph", Am. Heart J., 49:336, (1955).
8. Abildskov, J.A., Hisey, B.L. and Ingerson, W.E., "The Magnitude and Orientation of Ventricular Excitation Vectors in the Normal Heart and Following Myocardial Infarction", Am. Heart J., 55:104, (1958).
9. Park, W.K.R., "A Polarcardiograph Computer", M.A.Sc. Thesis, University of British Columbia, (1954).
10. Poole, E.G., "A Spherical Polarcardiograph Computer", M.A.Sc. Thesis, University of British Columbia, (1955).
11. Frank, E., "An Accurate, Clinically Practical System for Spatial Vectorcardiograph", Circulation, 13:737, (1956).
12. Dower, G.E., and Osborne, J.A., "A Clinical Comparison of Three VCG Lead Systems Using Resistance-combining Networks", Am. Heart J., 55:523, (1958).

13. Hilbiber, D.F., "A New DC Transistor Differential Amplifier",
Trans. IRE, CT-8:434-439, (December, 1961).
14. Friedberg, C.F., "Diseases of the Heart", W.B. Saunders Co.,
Philadelphia, Pa., p. 324, (1956).